This article is published as part of the *Dalton Transactions* themed issue entitled:

Pincers and other hemilabile ligands

Guest Editors Dr Bert Klein Gebbink and Gerard van Koten

Published in issue 35, 2011 of *Dalton Transactions*

Image reproduced with permission of Jun-Fang Gong

Articles in the issue include:

PERSPECTIVE:

ARTICLES:

Dalton Transactions

Dynamic Article Links

Cite this: *Dalton Trans.*, 2011, **40**, 8922

www.rsc.org/dalton

PAPER

OCO and NCO chelated derivatives of heavier group 15 elements. Study on possibility of cyclization reaction *via* intramolecular ether bond cleavage†

Libor Dostál,*[a] Roman Jambor,[a] Aleš Růžička,[a] Robert Jirásko,[b] Jaroslav Holeček[a] and Frank De Proft[c]

Received 11th February 2011, Accepted 10th March 2011
DOI: 10.1039/c1dt10234f

A set of four pincer ligands, either the OCO type ligands L^{1-3} [2,6-$(ROCH_2)_2C_6H_3$]$^-$, where R = Me (L^1), mesityl (L^2), *t*-Bu (L^3) or novel NCO ligand [2-(Me_2NCH_2)-6-(*t*-$BuOCH_2)C_6H_3$]$^-$ was studied. The reaction of L^4Li with PCl_3 resulted in isolation of [2-(OCH_2)-6-$(Me_2NCH_2)C_6H_3$]PCl (**1**) as a result of intramolecular ether bond cleavage and elimination of *t*-BuCl. The conversion between the organolithium compounds $L^{1,2,4}Li$ and $AsCl_3$ led to the desired chlorides, *i.e.* $(L^1)_2AsCl$ (**2**), L^2AsCl_2 (**3**), L^4AsCl_2 (**5**), but an analogous reaction using the L^3Li compound gave [2-(OCH_2)-6-(*t*-$BuOCH_2)C_6H_3$]AsCl (**4**) as a result of intramolecular cyclization. The organoantimony chloride L^3SbCl_2 was shown to undergo very slow cyclization in $CDCl_3$ again *via* elimination of *t*-BuCl giving [2-(OCH_2)-6-(*t*-$BuOCH_2)C_6H_3$]SbCl (**6**) and it was demonstrated that this reaction may be accelerated by preparation of $L^3Sb(Cl)(OTf)$ (**7**) with more Lewis acidic central atom. On the contrary, both antimony derivatives of the NCO ligand L^4, not only the chloride L^4SbCl_2 (**8**) but also the ionic pair containing highly Lewis acidic cation $[L^4SbCl]^+[CB_{11}H_{12}]^-$ (**9**), are stable without any indication for etheral bond cleavage. The situation is rather similar in the case of organobismuth derivatives of L^4, which allowed isolation of compounds L^4BiCl_2 (**10**), $L^4Bi(Cl)(OTf)$ (**11**) and $[L^4BiCl]^+[CB_{11}H_{12}]^-$ (**12**). All studied compounds were characterized by the help of ^1H and ^{13}C NMR spectroscopy, ESI mass spectrometry, elemental analysis and (except **1**) by single-crystal X-ray diffraction.

Introduction

The chemistry of potentially terdentate, so-called pincer[1] type, ligands has developed into a well established branch of organometallic chemistry during the last four decades, which has been continuously reviewed.[2] The majority of ligands contained nitrogen[3] or phosphorus[4] atoms as inbuilt donor centers, but ligands using other donor atoms such as S, As, Se, or even carbenes emerged.[5] On the contrary, ligands based on an oxygen donor were not used. In 1998,[6] Jurkschat *et al.* enriched the pincer family by the introduction of the OCO ligand, $\{4\text{-}t\text{-Bu-2,6-}[P(O)(OR)_2]_2C_6H_2\}^-$ (R = Et or *i*-Pr). The chemistry of this ligand has been extended to Li, Si, Sn and Pb up to now.[7] The intramolecular cyclization reaction[8] is one of the most interesting results, which has been obtained in the course of the investigation of OCO chelated main group element compounds (Scheme 1). This type of reaction

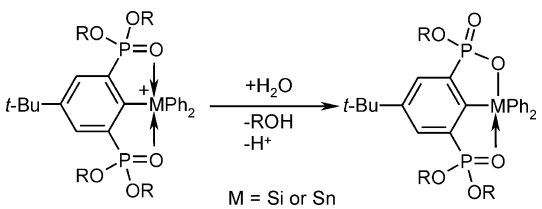

Scheme 1

resulted to closure of five-membered cycles, in which the central atoms are connected to oxygen atoms by a single covalent bond instead of a M←O dative interaction. This cyclization suggested, although other possibilities are also available, generation of organometallic cations as strong Lewis acids. From these studies, one may conclude that the central atom has to possess sufficient Lewis acidity to undergo such cyclization.

Of note, Veige *et al.* have reported on utilization of an interesting trianionic OCO pincer ligand recently, where two metallacycles are formed with the central atom.[9] Vicente *et al.* also described utilization of a 2,6-dinitroaryl ligand as a OCO pincer.[10]

Non-symmetrically substituted pincer type ligands containing two different coordinating ligand arms (especially NCP, OCS and OCP types) were described as well.[11] The unique coordination environment provided by these unsymmetric pincer ligands enabled new modes of reactivity.[2d,12]

[a]*Department of General and Inorganic Chemistry, Faculty of Chemical Technology, University of Pardubice, Studentská 573, CZ - 532 10, Pardubice, Czech Republic. E-mail: libor.dostal@upce.cz; Fax: +420466037068; Tel: +420466037163*

[b]*Department of Analytical Chemistry, Faculty of Chemical Technology, University of Pardubice, Studentská 573, CZ - 532 10, Pardubice, Czech Republic*

[c]*Eenheid Algemene Chemie (ALGC), Vrije Universiteit Brussel (VUB), Pleinlaan 2, B-1050, Brussels, Belgium*

† CCDC reference numbers 801796–801806. For crystallographic data in CIF or other electronic format see DOI: 10.1039/c1dt10234f

We reported on OCO pincer type ligands based on ether donor groups in 2002[13] (Fig. 1A) and developed their chemistry to other main group elements.[14] However, significant problems were met during reactions of lithium precursors with strong Lewis acids *e.g.* $AlCl_3$, $SiCl_4$ or $SnCl_4$, and desired products were not isolated, or adducts such as $AlCl_3 \cdot Et_3N$ had to be used for successful syntheses.[15] On the contrary, we have demonstrated that OCO chelating ligands L^{1-3} (Fig. 1A) may be used for stabilization of organoantimony halides of the type $L^{1-3}SbX_2$ (X = F, Cl, or I).[14a,f] Significant differences in behaviour of L^1 and L^3 were obtained, when the Lewis acidity of the antimony atom was increased. While the L^1 ligand is able to stabilize organoantimony cations or triflates $[L^1SbCl]^+[X]^-$ (X = OTf or $CB_{11}H_{12}$) (Fig. 2A),[16] significant problems were met in similar reactions with the ligand L^3. Thus, use of the ligand L^3 resulted in mixtures of products, probably due to an intramolecular ether bond cleavage since the *t*-Bu group in L^3 should be a significantly better leaving group than methyl in the case of the ligand L^1.[16]

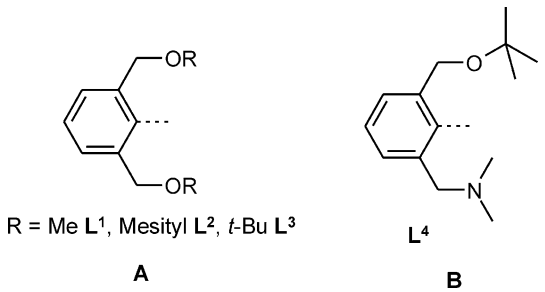

Fig. 1

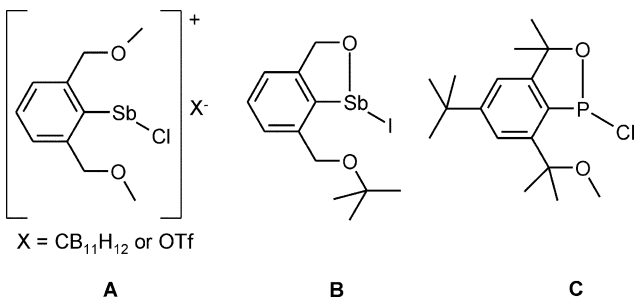

Fig. 2

These conclusions were often supported by results obtained by electrospray ionization (ESI) mass spectra of OCO chelated organometallic compounds. Especially, the tandem mass spectra of the ions containing OCO ligands showed further fragmentation of the CH_2OR pendant arms of the ligands, thus in most cases alkene losses for *tert*-butyl and isopropyl substituted ligands were detected, whereas alcohol or aldehyde losses were preferred for methyl and ethyl substitution of a pincer ligand. It is also noteworthy, that the neutral loss of butene is even observed in full scan mass spectra for most of organometallic compounds that contain OCO ligands with *t*-Bu groups (L^3) (Fig. 1A).[17]

It has been shown recently that the reaction of organoantimony sulfide $[L^3SbS]_2$ with iodine gave an oxastibol (Fig. 2B) as a side product. In this compound, one of the *t*-Bu groups was eliminated from the molecule under formation of a new Sb–O covalent bond and closure of a five-membered oxastibol ring.[18] This finding proved the possibility of intramolecular bond disruption and cyclization in the case of organometallic compounds containing OCO pincer type ligands (Fig. 1A) and prompted us to study this phenomenon in more detail.

As a part of these studies, we report here on experimental investigation dealing with possible cyclization reactions in the series of group 15 element (P to Bi) compounds containing ligands L^{1-4} (Fig. 1A, B). The utilization of these four ligands enables us to follow two basic trends: (i) varying substituents on the etheral oxygen atoms in the ligands L^{1-3}; (ii) influence of the presence of the nitrogen donor atom in the ligand L^4. This ligand is purposely substituted by the *t*-Bu group on the etheral oxygen atom, since the *t*-Bu group is believed to be the best leaving group in the cyclization reaction. All studied compounds **1–12** (Schemes 2–5) were characterized by the help of multinuclear NMR spectroscopy, ESI mass spectrometry, and except the compound **1** (oil), by X-ray diffraction.

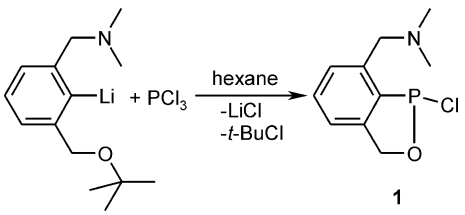

Scheme 2

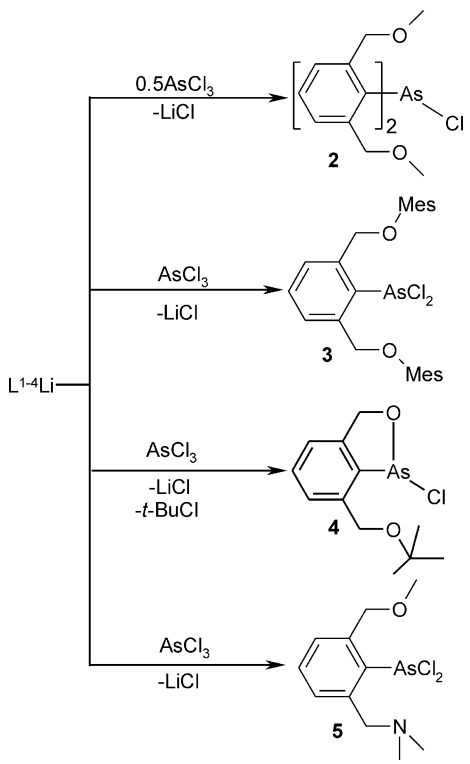

Scheme 3

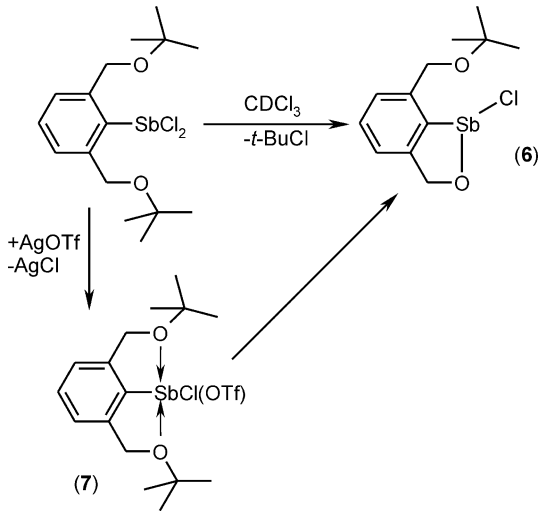

Scheme 4

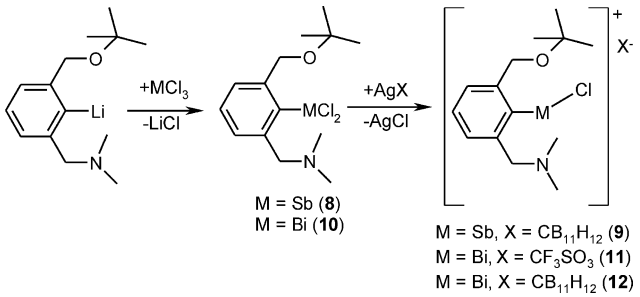

Scheme 5

Results and discussion

The discussion is arranged consecutively according to the central atom used. New compounds are numbered and their syntheses are described in detail in the Experimental section. Compounds that have been already published, are not numbered, but are described by their formulas and cited in references.

Organophosphorus compounds

The cyclization among similar OCO and CO chelated organophosphorus compounds has recently been studied in detail by Yoshifuji.[19] These studies showed that the organophosphorus dichlorides smoothly undergo intramolecular cyclization with concomitant elimination of an alkyl chloride yielding compounds with a covalent P–O bond (Fig. 2C). However, when an aryl was used as the substituent on the etheral oxygen atom no cleavage of the ether bond is observed. This difference was ascribed to a change of the hybridization of the carbon atom from sp^3 (alkyl) to sp^2 (aryl). These results well coincide with our findings on OCO ligands L^2 and L^3, thus the compound L^3PCl_2 is not isolable and readily eliminates *t*-BuCl to give a five-membered C_3PO ring, while compound L^2PCl_2 is stable.[20]

Similarly, the reaction of L^4Li with PCl_3 led to the cyclized product **1** in good yield (Scheme 2). The ^{31}P NMR spectrum of **1** revealed one signal at 165.9 ppm and this value well corresponds to that at 172.6 ppm for an OCO-cyclized analogue.[20] The signal of the *t*-Bu moiety is absent in the ^1H NMR spectra also proving elimination of *t*-BuCl in the course of the reaction (Scheme 2). This fact points to the same behaviour of the NCO chelated compound in comparison with OCO ones. The P←N coordination most probably does not saturate the Lewis acidic phosphorus atom enough, so leading to cyclization, and this finding also establishes that the *t*-Bu moiety is a good leaving group in this cyclization.

Organoarsenic compounds

Albeit OCO chelated organophosphorus compounds were studied in detail in the past, similar organoarsenic compounds are unknown. Thus, reactions of $L^{1-4}Li$ with $AsCl_3$ were studied to obtain OCO chelated organoarsenic chlorides (Scheme 3). The reaction between L^1Li and $AsCl_3$ gave diorganoarsenic compound $(L^1)_2AsCl$ (**2**) as the only isolable product regardless on the molar L^1 : As ratio used (1 : 1 or 2 : 1), the second variant, however, giving better yields of **2**. The ^1H NMR spectra of **2** contains an AB pattern (4.48 ppm) for OCH_2 groups and a signal at 3.21 ppm for CH_3O moieties, indicating fluxional behaviour of **2** in solution. The reaction of L^2Li and $AsCl_3$ gave desired L^2AsCl_2 (**3**) in good yield, as demonstrated by ^1H and ^{13}C NMR spectra. The ^1H NMR spectrum contains only one sharp signal for the OCH_2 moiety (5.35 ppm) indicating most probably again fluxional behaviour in solution (coordination/de-coordination of ligands arms), because only one of the ligand's arms is coordinated to the central arsenic atom in the solid state (*vide infra*). Of note, treatment of L^3Li with one molar equivalent of $AsCl_3$ led to the elimination of *t*-BuCl and isolation of the cyclized product [2-(OCH_2)-6-(*t*-$BuOCH_2)C_6H_3$]AsCl (**4**). This fact was clearly demonstrated by the ^1H NMR spectrum of **4**, which contains two signals for OCH_2 moieties (4.76 and 5.56 ppm in 2 : 2 integral ratio) and only one signal for *t*-BuO group (integral intensity 9). Three signals (1 : 1 : 1 ratio) are observed in the aromatic region of the ^1H NMR spectrum of **4**. These findings well correspond to those observed in the case of OCO coordinated organophosphorus compounds. Finally, using ligand L^4, bearing a nitrogen donor centre, allowed synthesis of the dichloride L^4AsCl_2 (**5**) and the *t*-BuO group remains intact in this compound, as revealed by ^1H and ^{13}C NMR spectra. This finding is notable and suggests that the presence of the nitrogen donor atom restrains the propensity of the *t*-BuO group to undergo cyclization in the case of **5**, in comparison to a smooth cyclization of one of the ligand's arms in compound **4**, where the OCO ligand L^3 was used.

The molecular structures of **2–5** were determined by single-crystal X-ray diffraction and are depicted in Fig. 3–6, relevant geometric parameters are given in the figures captions and the crystallographic data are summarized in the Experimental section.

Only one of four oxygen atoms of ligands L^1 (Fig. 3) is coordinated to the arsenic atom in **2** as demonstrated by the bond length As(1)–O(1) 2.610(6) Å (d_{vdW}(As,O) = 3.37, d_{cov}(As,O) = 1.89 Å). The coordination polyhedron of the arsenic atom As(1) in **2** can be described as a distorted vacant trigonal bipyramid as a result of this intramolecular As–O contact. The oxygen atom O(1) and the chlorine atom Cl(1) are located in the axial positions with the angle Cl(1)–As(1)–O(1) 162.6(2)°. The equatorial positions are occupied by two *ipso* carbon atoms C(1) and C(11) and the third position is most probably filled by the arsenic lone pair leading to the narrowing of the bonding angle C(1)–As(1)–C(11) to 104.3(3)° from an ideal value 120° for a trigonal-pyramidal environment.

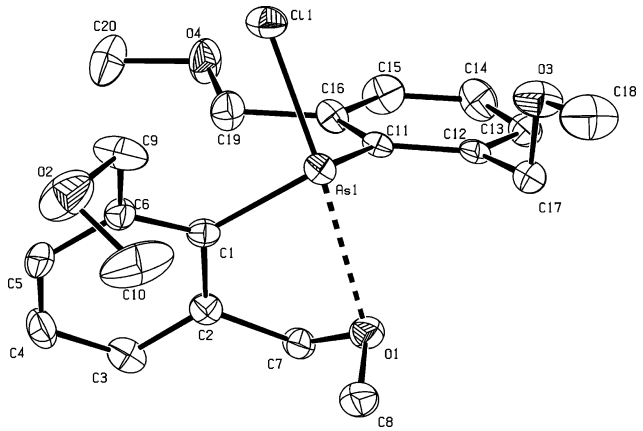

Fig. 3 Molecular structure of **2** (ORTEP drawing with 30% probability ellipsoids) with the labelling scheme. Hydrogen atoms have been omitted for clarity. Selected bond lengths (Å) and angles (°): As(1)–C(1) 1.971(7), As(1)–C(11) 1.993(7), As(1)–O(1) 2.610(6), As(1)–O(3) 3.322(8), As(1)–Cl(1) 2.259(2); C(1)–As(1)–C(11) 104.3(3), Cl(1)–As(1)–O(1) 162.6(2), C(1)–As(1)–Cl(1) 99.1(2), C(11)–As(1)–Cl(1) 91.1(2), C(1)–As(1)–O(1) 74.0(2), C(11)–As(1)–O(1) 75.6(3).

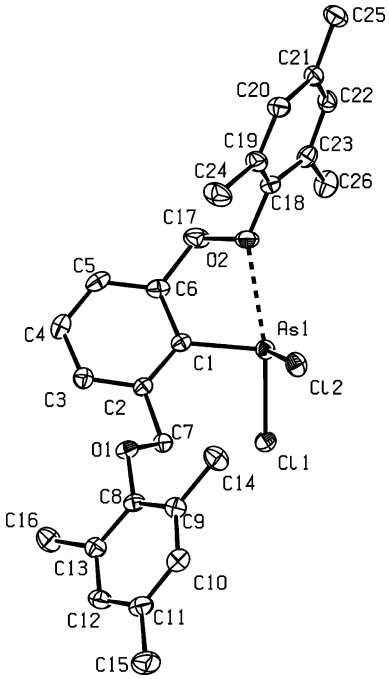

Fig. 4 Molecular structure of **3** (ORTEP drawing with 30% probability ellipsoids) with the labelling scheme. Hydrogen atoms have been omitted for clarity. Selected bond lengths (Å) and angles (°): As(1)–C(1) 1.958(2), As(1)–O(2) 2.5907(18), As(1)–Cl(1) 2.2259(7), As(1)–Cl(2) 2.2034(7); C(1)–As(1)–Cl(1) 97.62(7), C(1)–As(1)–Cl(2) 100.18(7), C(1)–As(1)–O(2) 74.73(8), Cl(1)–As(1)–O(2) 166.83(4), Cl(2)–As(1)–O(2) 93.20(5).

The coordination polyhedron of the central atom in **3** (Fig. 4) resembles that found in compound **2**, *i.e.* a distorted vacant trigonal bipyramid, but the molecular structure of **3** contains two chlorine atoms instead of two ligands in comparison to **2**. Again only one of the oxygen atoms, O(2), is coordinated to As(1) with a bond length As(1)–O(2) 2.5907(18) Å. This distance is slightly shorter than that in **2** (2.610(6) Å) reflecting higher Lewis acidity of the central atom. The donor atoms O(2) and Cl(1) atom occupy

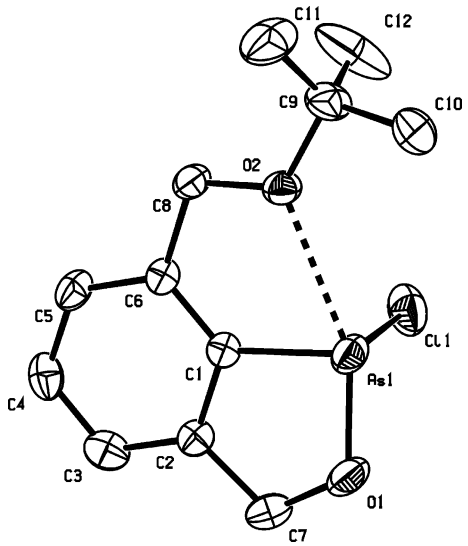

Fig. 5 Molecular structure of **4** (ORTEP drawing with 30% probability ellipsoids) with the labelling scheme. Hydrogen atoms have been omitted for clarity. Selected bond lengths (Å) and angles (°): As(1)–C(1) 1.903(5), As(1)–O(1) 1.786(4), As(1)–O(2) 2.627(3), As(1)–Cl(1) 2.262(2); C(1)–As(1)–Cl(1) 94.86(17), O(1)–As(1)–O(2) 157.13(18), Cl(1)–As(1)–O(1) 98.95(15), Cl(1)–As(1)–O(2) 92.02(10), C(1)–As(1)–O(1) 88.5(2), C(1)–As(1)–O(2) 70.53(18).

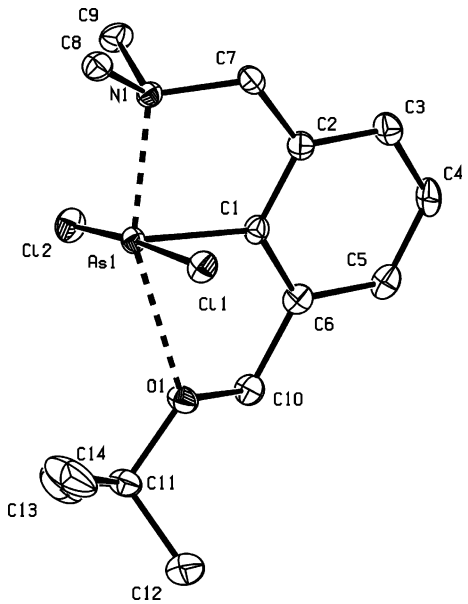

Fig. 6 Molecular structure of **5** (ORTEP drawing with 30% probability ellipsoids) with the labelling scheme. Hydrogen atoms have been omitted for clarity. Selected bond lengths (Å) and angles (°): As(1)–C(1) 1.928(3), As(1)–N(1) 2.131(3), As(1)–O(1) 2.487(2), As(1)–Cl(1) 2.5143(11), As(1)–Cl(2) 2.4470(10); N(1)–As(1)–O(1) 155.73(11), Cl(1)–As(1)–Cl(2) 175.88(2), C(1)–As(1)–N(1) 82.75(13), C(1)–As(1)–O(1) 73.06(12), C(1)–As(1)–Cl(1) 89.28(10), C(1)–As(1)–Cl(2) 89.18(10).

axial positions (bonding angle Cl(1)–As(1)–O(2) 166.83(4)°) and the equatorial plane is formed by the C(1), Cl(2) atoms (angle C(1)–As(1)–Cl(2) 100.18(7)°) and the lone pair of the arsenic atom.

Determination of the molecular structure of **4** (Fig. 5) proved the proposed structure, in which one of the ligand arms of L^3 is broken under elimination of *t*-BuCl leading to formation of a new

As–O bond and closure of a five-membered oxa-arsa ring system. The bond length As(1)–O(1) is 1.786(4) Å and corresponds well to the value for a As–O covalent bond (d_{cov}(As,O) = 1.89 Å). The second arm of the ligand remains intact and is coordinated to the central atom with bond distance As(1)–O(2) 2.627(3) Å and this value resembles those found in **2** and **3**. The value of the bonding angle O(1)–As(1)–O(2), although the oxygen atoms are coordinated formally in the apical positions of a distorted vacant trigonal bipyramid, is highly acute 157.13(18)° and this must be ascribed to the ring strain of the oxa-arsa ring. The molecular structure of **4** remains essentially monomeric without any significant intermolecular contact, which is in a sharp contrast to antimony analogues (Fig. 2B)[18] and **6** with the tetrameric structure *vide infra*.

Both donor atoms, the oxygen atom O(1) as well as nitrogen atom N(1), are coordinated to the central arsenic atom As(1) with bond distances As(1)–O(1) 2.487(2) and As(1)–N(1) 2.131(3) Å in the molecular structure of **5** (Fig. 6). These dative coordinations lead to a distorted tetragonal pyramidal shape of the coordination polyhedron of the central As(1) atom. The basal plane is formed by the donor atoms (N(1) and O(1)) and both chlorine atoms, which are both coordinated mutually in a pseudo-*trans* fashion with bonding angles N(1)–As(1)–O(1) 155.73(11) and Cl(1)–As(1)–Cl(2) 175.88(2)°. The apex is occupied by the *ipso* carbon atom C(1). This type of environment is very typical for dihalogeno-OCO and -NCN pincer type antimony and bismuth compounds.[14a,21]

Organoantimony compounds

As mentioned in the introduction, different behaviour of ligands L^1 and L^3 was observed in organoantimony cations[16] and this fact made us study organoantimony compounds containing the ligand L^3 in more detail. The chloride L^3SbCl_2 is stable in the solid state for several months and in $CDCl_3$ solution for a period of several weeks.[14a] Nevertheless, very slow cyclization of L^3SbCl_2 with concomitant elimination of *t*-BuCl, yielding compound [2-(OCH_2)-6-(*t*-BuOCH_2)C_6H_3]SbCl (**6**), was observed in $CDCl_3$ solution and was monitored by ^{1}H NMR spectroscopy (Scheme 4). The ^{1}H NMR spectrum of L^3SbCl_2 contains one signal for OCH_2 moieties at 5.03 ppm, but upon standing in $CDCl_3$ solution at ambient temperature two additional singlets for OCH_2 groups (4.77 and 5.63 ppm, 2 : 2 integral ratio) and one singlet for *t*-BuO group (1.47 ppm, integral intensity 9) emerged, pointing to formation of **6**. These signals increased in their intensity giving *ca.* 60% conversion after 6 months. Attempts to accelerate this reaction by heating were hampered in part by decomposition and hydrolysis leading to a mixture of decomposition products. According with the idea that the cyclization is caused by Lewis acidity of the central antimony atom, one of the chlorine atoms in L^3SbCl_2 was substituted by a triflate group by reaction with silver triflate to give $L^3SbCl(OTf)$ (**7**). The ^{1}H NMR spectrum of **7** contains sharp signals for both OCH_2 and CH_3O groups (5.17 and 1.70 ppm, respectively). The presence of the OTf group was established also by observation of a quartet in the ^{13}C NMR spectrum at 119.7 ppm ($^1J(^{13}C,^{19}F) = 318$ Hz). The increased Lewis acidity of the antimony atom in **7** accelerates the cyclization process and full conversion to compound **6** can be observed typically in only 6–7 days in $CDCl_3$ solution (Scheme 4).

Using ligand L^4 (Scheme 5) allowed isolation of the chloride L^4SbCl_2 (**8**), that showed no propensity to cyclization, and an even more stable ionic compound $[L^4SbCl]^+[CB_{11}H_{12}]^-$ (**9**) was prepared, that is stable in solution for several weeks. The stability of both compounds in comparison to OCO chelated analogues L^3SbCl_2 and **7** is most probably again the result of the amino pendant arm, which more effectively saturates the antimony centre in comparison to two ethereal donor centers in the case of the ligand L^3.

The molecular structures of **6–9** are shown in Fig. 7–10 together with relevant structural parameters. In contrast to the monomeric structure of the arsenic analogue **4**, compound **6** forms a relatively tightly bonded cyclic tetramer, due to significant intermolecular Sb–O contacts. It is evident that one of the ligand arms on each ligand was cleaved under formation of a new Sb–O covalent bond. The bond distances are Sb(1)–O(2) 2.045(4), Sb(2)–O(4) 2.050(5), Sb(3)–O(6) 2.045(4) and Sb(4)–O(8) 2.037(5) Å and well correspond to d_{cov}(Sb,O) = 2.02 Å. The second arm of each ligand (oxygen atoms O(1), O(3), O(5) and O(7)) remains intact but still show significant contact with central antimony atoms (range of bond distances 2.605(5)–2.593(7) Å). The coordination

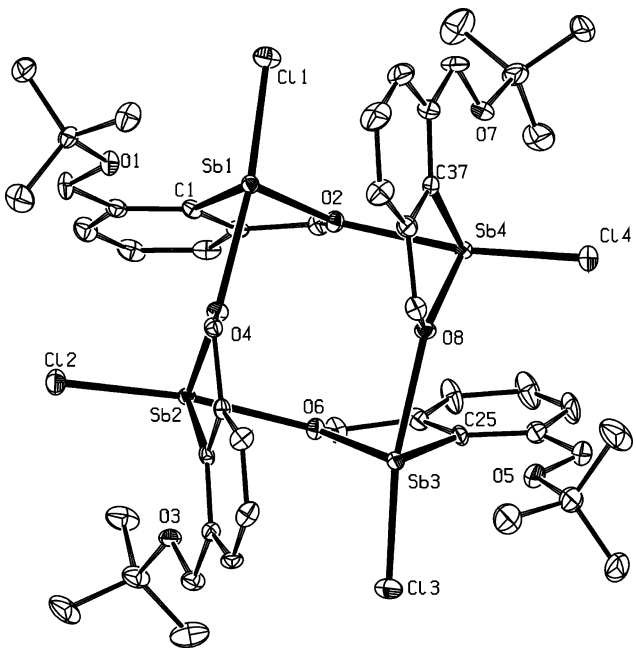

Fig. 7 Molecular structure of **6** (ORTEP drawing with 30% probability ellipsoids) with the labelling scheme. Hydrogen atoms have been omitted for clarity. Selected bond lengths (Å) and angles (°): Sb(1)–C(1) 2.109(8), Sb(1)–Cl(1) 2.457(3), Sb(1)–O(1) 2.600(5), Sb(1)–O(2) 2.045(4), Sb(2)–C(13) 2.117(6), Sb(2)–Cl(2) 2.476(2), Sb(2)–O(3) 2.605(5), Sb(2)–O(4) 2.050(5), Sb(3)–C(25) 2.103(9), Sb(3)–Cl(3) 2.441(3), Sb(3)–O(5) 2.593(7), Sb(3)–O(6) 2.045(4), Sb(4)–C(37) 2.093(6), Sb(4)–Cl(4) 2.464(3), Sb(4)–O(7) 2.599(6), Sb(4)–O(8) 2.037(5), Sb(1)–O(4) 2.444(6), Sb(2)–O(6) 2.432(5), Sb(3)–O(8) 2.477(6), Sb(4)–O(2) 2.485(5); O(1)–Sb(1)–O(2) 148.51(18), Cl(1)–Sb(1)–O(4) 170.38(13), O(3)–Sb(2)–O(4) 148.61(14), Cl(2)–Sb(2)–O(6) 170.24(12), O(5)–Sb(3)–O(6) 148.4(2), Cl(3)–Sb(3)–O(8) 168.31(14), O(7)–Sb(4)–O(8) 149.23(17), Cl(4)–Sb(4)–O(2) 168.60(12), O(2)–Sb(1)–O(4) 89.36(19), Sb(1)–O(4)–Sb(2) 130.68(18), O(4)–Sb(2)–O(6) 90.60(19), Sb(2)–O(6)–Sb(3) 130.93(19), O(6)–Sb(3)–O(8) 90.39(19), Sb(3)–O(8)–Sb(4) 130.06(18), O(8)–Sb(4)–O(2) 89.12(19), Sb(4)–O(2)–Sb(1) 128.8(2).

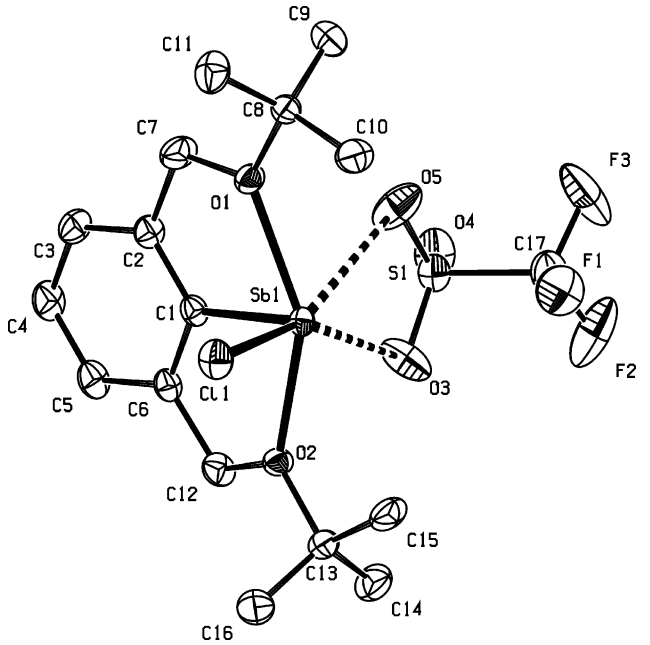

Fig. 8 Molecular structure of **7** (ORTEP drawing with 30% probability ellipsoids) with the labelling scheme. Hydrogen atoms have been omitted for clarity. Selected bond lengths (Å) and angles (°): Sb(1)–C(1) 2.093(3), Sb(1)–Cl(1) 2.3950(10), Sb(1)–O(1) 2.312(2), Sb(1)–O(2) 2.275(2), Sb(1)–O(3) 2.971(3), Sb(1)–O(5) 2.998(3); C(1)–Sb(1)–O(1) 74.37(11), C(1)–Sb(1)–O(2) 75.31(11), C(1)–Sb(1)–O(3) 85.01(11), C(1)–Sb(1)–O(5) 85.29(11), C(1)–Sb(1)–Cl(1) 95.56(9), Cl(1)–Sb(1)–O(1) 86.72(6), O(1)–Sb(1)–O(5) 72.49(9), O(5)–Sb(1)–O(3) 46.11(10), O(3)–Sb(1)–O(2) 68.49(9), O(2)–Sb(1)–Cl(1) 68.49(9).

polyhedron at each antimony atom Sb(1–4) may be best described as a strongly distorted tetragonal pyramid, with the *ipso* carbon atoms in the axial position, as a result of a additional intermolecular contact with the oxygen atoms of the neighboring molecule, *e.g.* the Sb(1)–O(4) contact. These intermolecular contacts fall within a narrow interval 2.432(5)–2.485(5) Å. Interestingly, these contacts are stronger than those found in the iodine analogue Fig. 2B. The resulting central Sb_4O_4 ring is strongly puckered as demonstrated by the selected bond angles, see figure caption.

The molecular structure of compound **7** (Fig. 8) is of particular interest in this study, because its structure may shed some light on the reason why this compound undergoes the cyclization reaction to **6** so smoothly, in comparison with the chloride L^3SbCl_2. The coordination number of the central atom Sb(1) is six and the coordination polyhedron may be best described as a strongly distorted pentagonal pyramid. This is a result of the rigid tridentate coordination of the pincer ligand (atoms C(1), O(1) and O(2)), bidentate coordination of the triflate moiety (O(3) and O(5)) and the sixth coordination place is occupied by the chlorine atom Cl(1). The heteroatoms form the basal plane and the carbon atom C(1) is located in the apical position. The triflate group is coordinated to the central atom very weakly as demonstrated by the bond distances Sb(1)–O(3) 2.971(3), Sb(1)–O(5) 2.998(3) Å, which are significantly longer than d_{cov}(Sb,O) = 2.02 Å, but still below the d_{vdW}(Sb,O) = 3.52 Å. In contrast, the intramolecular Sb–O(pincer) dative interactions (Sb(1)–O(1) 2.312(2), Sb(1)–O(2) 2.275(2) Å) are the strongest observed by us so far among all organoantimony derivatives of L^3; the corresponding values in

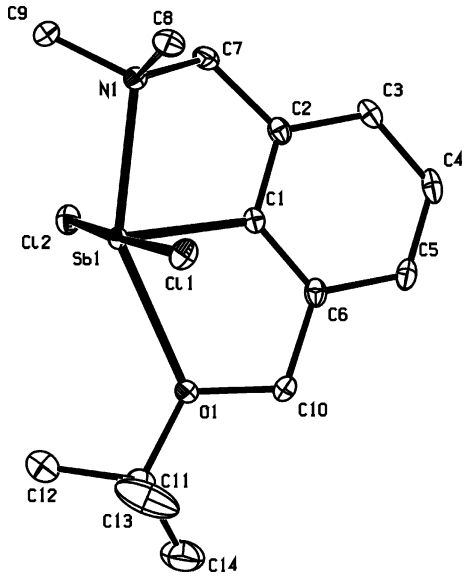

Fig. 9 Molecular structure of **8** (ORTEP drawing with 30% probability ellipsoids) with the labelling scheme. Hydrogen atoms have been omitted for clarity. Selected bond lengths (Å) and angles (°): Sb(1)–C(1) 2.104(3), Sb(1)–N(1) 2.336(3), Sb(1)–O(1) 2.485(2), Sb(1)–Cl(1) 2.5846(14), Sb(1)–Cl(2) 2.6174(14); C(1)–Sb(1)–N(1) 77.36(12), C(1)–Sb(1)–O(1) 70.86(12), C(1)–Sb(1)–Cl(1) 87.44(9), C(1)–Sb(1)–Cl(2) 86.94(9), N(1)–Sb(1)–O(1) 148.22(11), Cl(1)–Sb(1)–Cl(2) 174.38(4).

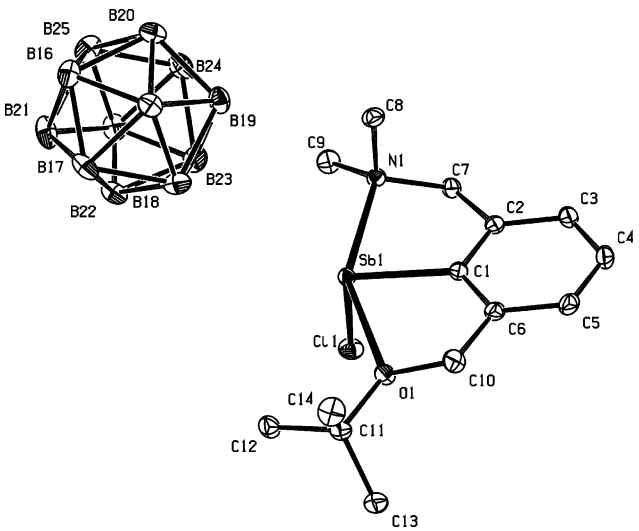

Fig. 10 Molecular structure of **9** (ORTEP drawing with 30% probability ellipsoids) with the labelling scheme. Hydrogen atoms have been omitted for clarity. Selected bond lengths (Å) and angles (°): Sb(1)–C(1) 2.101(2), Sb(1)–N(1) 2.2881(17), Sb(1)–O(1) 2.4706(15), Sb(1)–Cl(1) 2.3668(6); C(1)–Sb(1)–N(1) 77.27(7), C(1)–Sb(1)–O(1) 71.50(7), C(1)–Sb(1)–Cl(1) 95.08(7), N(1)–Sb(1)–O(1) 148.68(6), N(1)–Sb(1)–Cl(1) 90.40(5), O(1)–Sb(1)–Cl(1) 94.57(4).

compound L^3SbCl_2 are 2.6911(13) and 2.6294(14) Å.[14a] Provided that we accept strong intramolecular interactions as a starting point for the cyclization process, the comparison of these Sb–O interactions clearly explains the relative ease of cyclization for compound **7** in comparison to the chloride L^3SbCl_2 (*vide supra*).

This conclusion seems to be even more valid in solution, where the triflate group may easily de-coordinate from the central atom and in such a way further increase the Lewis acidity of the central atom in **7**. Strengthening of the Sb–O interaction is expected which will promote the cyclization.

Other aspects are also relevant in this discussion. The closest values of Sb–O intramolecular interactions to those in **7** were observed in the compound L^3SbI_2 (2.302(2) and 2.343(2) Å),[14a] a formal precursor of the only cyclized product (Fig. 2B) reported to date, thus confirming our idea. Moreover, in the cation of ionic pairs containing the ligand L^1 (Fig. 1A), such as $[L^1SbCl]^+[CB_{11}H_{12}]^-$, and the corresponding triflates[16] the Sb–O interactions are in the range 2.226(7)–2.324(4) Å, thus comparable to the values in **7**. Nevertheless, the methyl groups on the ligand arms in the ligand L^1 remained intact proving that the propensity of *t*-Bu group (L^3) elimination is easier than elimination of the methyl groups in L^1. Finally, in the case of *t*-Bu substituted NCO ligand L^4 the oxygen containing ligand arm is not cleaved even in the ionic pair $[L^4SbCl]^+[CB_{11}H_{12}]^-$ **9** (for description of its molecular structure see below). Also the Sb–O bond distance is quite long 2.4706(15) Å in **9** most probably as a result of an effective saturation of the central antimony atom by the N-donor ligand arm. This fact may point to the conclusion that the cleavage of the etheral bond will be more feasible in the case of OCO than in NCO ligands.

The molecular structure of compound **8** is shown in Fig. 9. In fact, this structure is closely related to the arsenic analogue L^4AsCl_2 **5**. Thus the coordination polyhedron of the central antimony atom may be defined as a strongly distorted tetragonal pyramid, where the basal plane is formed by two chlorine atoms in a *trans* orientation, Cl(1)–Sb(1)–Cl(2) 174.38(4)°, and the donor atoms N(1) and O(1) (angle N(1)–Sb(1)–O(1) 148.22(11)°). The apex is occupied by the *ipso* carbon atom C(1). Concerning the Sb–O interaction as the main important structural feature (Sb(1)–O(1) 2.485(2) Å), the coordination is stronger than found in L^3SbCl_2. This result seems to contradict the fact that nitrogen atoms saturate the central metal more efficiently and so weaker Sb–O interaction in **8** might be expected in comparison to the OCO chelated L^3SbCl_2. However, the strengthening of the Sb–O interaction in **8** can be ascribed to a change in the ligand coordination geometry from pseudo-facial in L^3SbCl_2 (O–Sb–O angle 116.73(4)°) to pseudo-meridional in **8** (N(1)–Sb(1)–O(1) 148.22(11)°).[21a]

Compound **9** forms a well separated ionic pair (Fig. 10). The structure of the cationic part of **9** is best described as a vacant trigonal bipyramid, where the apical positions are occupied by the donor atoms N(1) and O(1) (angle N(1)–Sb(1)–O(1) 148.68(6)°). The intramolecular Sb(1)–N(1) interaction 2.2881(17) Å is, interestingly, slightly shorter in comparison to the analogous purely NCN chelated organoantimony cation (Sb–N bond distances 2.379(5) and 2.442(4) Å).[22] This fact again points to the conclusion that due to the very strong Sb–N intramolecular interaction in the NCO (ligand L^4) derivatives, the nitrogen donor atom provides a high level of saturation of the Lewis acidic central antimony atom leaving the Sb–O coordination as not so crucial for the stabilization of the cation (*cf.* Sb(1)–O(1) 2.4706(15) Å distance in **9** is apparently weaker than in analogous OCO chelated compounds such as in **7**, 2.312(2) and 2.275(2) Å).

Organobismuth compounds

The situation in the case of organobismuth derivatives is not so complicated in comparison with the antimony analogues. The OCO chelated organobismuth cation was shown to be stable in the compound $[L^3BiCl]^+[CB_{11}H_{12}]^-$.[16] Analogously, the bismuth compound L^4BiCl_2 (**10**) can be prepared as a stable solid and was characterized by ^1H and ^{13}C NMR spectra, where only one sharp signal is obtained for both OCH_2 and NCH_2 groups (4.78 and 5.08 ppm). Conversion of **10** with silver salts of polar groups gave compounds $L^4BiCl(OTf)$ (**11**) and $[L^4BiCl]^+[CB_{11}H_{12}]^-$ (**12**) (Scheme 5). Both compounds are stable in solution for extended times without any indication for a cyclization process.

Molecular structures of **10–12** are illustrated in Fig. 11–13 with selected structural parameters given in the figure captions. The structure of the NCO chelated organobismuth chloride **10** is depicted in Fig. 11. The coordination polyhedron is rather similar to the arsenic (**5**) and antimony (**8**) analogues, *i.e.* a strongly distorted tetragonal pyramid as a consequence of meridional coordination of the pincer ligand L^4. Of note, there is an additional intermolecular contact of 3.618(2) Å between the central atom Bi(1) and the chlorine tom Cl(1a) from the adjacent molecule Bi(1)–Cl(1a) (d_{vdW}(Bi,Cl) = 4.09 Å) leading to a very weakly coordinated dimeric unit in the solid state. This finding reflects the preference of the bismuth atom to adopt higher coordination numbers in comparison to lighter group 15 analogues as reported for similar compounds previously.[14a]

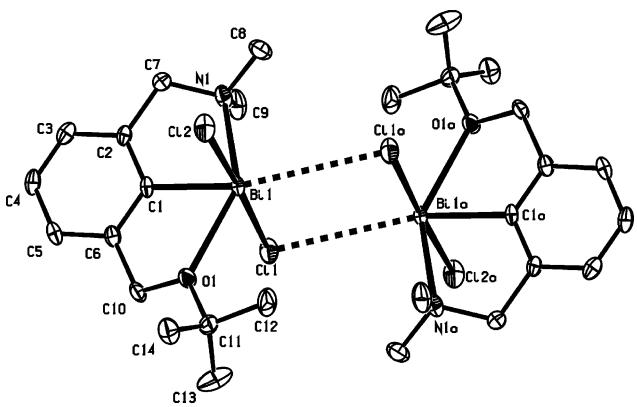

Fig. 11 Molecular structure of **10** (ORTEP drawing with 30% probability ellipsoids) with the labelling scheme. Hydrogen atoms have been omitted for clarity. a = 1 – *x*, 1 – *y*, –*z*. Selected bond lengths (Å) and angles (°): Bi(1)–C(1) 2.207(6), Bi(1)–N(1) 2.429(8), Bi(1)–O(1) 2.556(6), Bi(1)–Cl(1) 2.733(3), Bi(1)–Cl(2) 2.644(3), Bi(1)–Cl(1a) 3.618(2); N(1)–Bi(1)–O(1) 143.5(2), Cl(1)–Bi(1)–Cl(2) 177.06(8), C(1)–Bi(1)–Cl(1a) 156.85(19).

The formally dimeric structure is retained also in the case of the compound **11** (Fig. 12), but now the bridges are formed by triflate groups. The triflate moieties are coordinated only very weakly as demostrated by bond distances Bi(1)–O(2) 2.665(10), Bi(1)–O(3b) 3.009(9), Bi(1)–O(4b) 3.372(10) Å (d_{cov}(Bi,O) = 2.10 Å, d_{vdW}(Bi,O) = 3.52 Å) similarly to the OCO chelated analogue **7**. This bonding situation may be thus described also as contact ion pairs, where two triflate anions are caught between two bismuth cations. The pincer ligands are coordinated in tridentate fashion with bond distances Bi(1)–N(1) 2.431(11), Bi(1)–O(1) 2.558(9) Å in a pseudo-meridional fashion. The coordination number of the

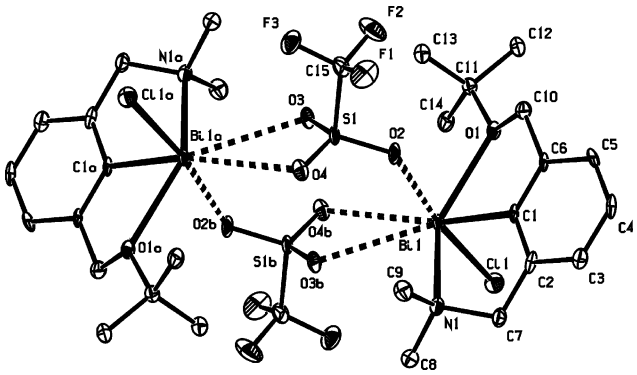

Fig. 12 Molecular structure of **11** (ORTEP drawing with 30% probability ellipsoids) with the labelling scheme. Hydrogen atoms have been omitted for clarity. a, b = 1 − *x*, −*y*, 1 − *z*. Selected bond lengths (Å) and angles (°): Bi(1)–C(1) 2.207(11), Bi(1)–N(1) 2.431(11), Bi(1)–O(1) 2.558(9), Bi(1)–Cl(1) 2.431(11), Bi(1)–O(2) 2.665(10), Bi(1)–O(3b) 3.009(9), Bi(1)–O(4b) 3.372(10); C(1)–Bi(1)–O(1) 69.4(5), C(1)–Bi(1)–N(1) 74.0(4), C(1)–Bi(1)–Cl(1) 91.9(3), C(1)–Bi(1)–O(2) 80.0(3), C(1)–Bi(1)–O(3b) 140.2(3), C(1)–Bi(1)–O(4b) 169.5(3).

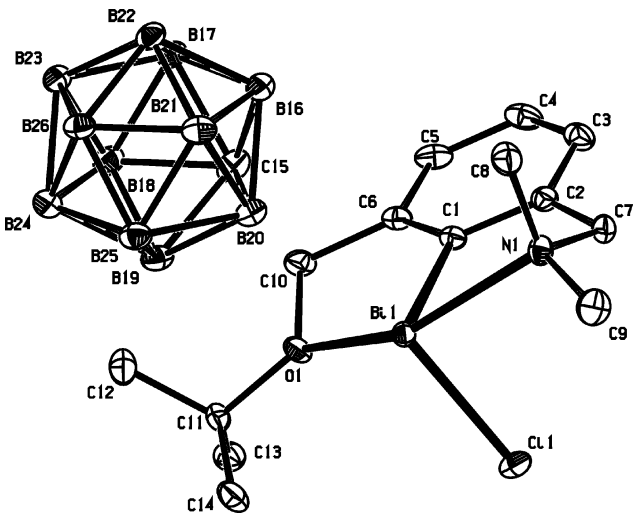

Fig. 13 Molecular structure of **12** (ORTEP drawing with 30% probability ellipsoids) with the labelling scheme. Hydrogen atoms have been omitted for clarity. a = 1 − *x*, −*y*, 1 − *z*. Selected bond lengths (Å) and angles (°): Bi(1)–C(1) 2.180(9), Bi(1)–N(1) 2.420(5), Bi(1)–O(1) 2.534(3), Bi(1)–Cl(1) 2.4819(12); C(1)–Bi(1)–N(1) 74.68(14), C(1)–Bi(1)–O(1) 69.54(14), C(1)–Bi(1)–Cl(1) 93.21(13), N(1)–Bi(1)–O(1) 144.21(11).

central bismuth atom is seven taking all the Bi–O(triflate) contacts into account.

Compound **12** forms an ionic pair (Fig. 13) similarly to the antimony analogue **9**. The vacant trigonal-bipyramidal array of the cation of **12** is built up by the pincer ligand (pseudo-meridional coordination with N(1)–Bi(1)–O(1) 144.21(11)°) and the chlorine atom Cl(1) occupying one of the equatorial positions. The values of the intramolecular interactions Bi(1)–N(1) 2.420(5), Bi(1)–O(1) 2.534(3) Å resemble those of analogous OCO and NCN chelated ionic pairs.[16,23]

Mass spectrometry

Tandem mass spectra of studied ions containing ligands L^{1-4} showed the neutral loss of $\Delta m/z$ 32 CH_3OH for **2**, $\Delta m/z$ 136 $C_9H_{11}OH$ for **3** and $\Delta m/z$ 56 C_4H_8 ($(CH_3)_2C{=}CH_2$). Major fragmentation mechanisms for other studied compounds containing ligands L^3 or L^4 were related to fragmentation of ligand arm with the *t*-Bu substituent on the oxygen atom. These finding proved the propensity of the oxygen containing ligand arm to be cleaved under the measurement conditions.

Theoretical considerations

Better insight into the cyclization behaviour of selected compounds can be obtained from theoretical calculations. Starting from the molecular structures, the compounds containing OCO and NCO ligands *i.e.* L^3MCl_2 and L^4MCl_2 (M = Sb and Bi) were fully optimized at the B3LYP[24]/cc-pVDZ[25] level (on Sb and Bi, the cc-pVDZ-PP basis set[26] was used) using the Gaussian 09 program.[27] Subsequent NBO analysis[28] reveals that in case of the L^4 ligand (NCO), an important interaction exists between the lone pairs on both oxygens and nitrogen and the formal empty p orbital on Sb and Bi, which coincides with strong intramolecular donor atom–metal interactions. Both structures can be approximately described by the formal formula $L^4M^{2+}Cl_2^{2-}$. In the case of OCO chelated L^3BiCl_2, there is a comparable interaction between the lone pairs on both oxygens with the formal empty p orbital on Bi and this compound can also be described as $L^3Bi^{2+}Cl_2^{2-}$. None of these three compounds is found to undergo cyclization. In the case of Sb congener L^3SbCl_2 however, this interaction is absent and an interaction exists between the oxygen lone pairs and the antibonding orbital of the Sb–Cl bonds. NBO analysis in this case clearly identifies two Sb–Cl bonds. This fact suggests that the cyclization process may be related to the nature of the metal–donor atom interaction. Thus interaction must not just be only between the lone pairs of donor atoms and empty orbitals of the central metal forming a Lewis pair. Electron density of the donor atoms can be, as shown by for example L^3SbCl_2, donated to antibonding orbitals of the compound backbone and such an interaction may be a impetus for cyclization.

Conclusions

The set of group 15 pincer compounds with one (L^4) or two (L^{1-3}) pendant CH_2OR groups was prepared, with the aim to follow the ability of this ligand arm to undergo intramolecular cyclization *via* ether bond disruption. Although, this set of compounds is still quite limited, the knowledge obtained in the course of this study enable us to make some preliminary conclusions for group 15 derivatives. (i) It is evident that the propensity to cyclization decreases from P to Bi, and no cyclization process was detected in the latter case. (ii) Regarding the structure of the oxygen ligand arm *i.e.* R group in CH_2OR, it seems that only the alkyl (sp^3 hybridized) substituents are prone to cyclization, especially the *t*-Bu group, because changing to aryl (mesityl, sp^2 hybridized) group gave stable products even with phosphorus as the central atom. (iii) The presence of the nitrogen pendant arm CH_2NMe_2 helps to prevent cyclization of CH_2Ot-Bu, thus for example the smooth cyclization reaction with arsenic chloride in the case of OCO ligand L^3 was not

observed in the case of NCO ligand L^4. Similarly, the cyclization may proceed in the case of OCO antimony compounds, but not for NCO ones. (iv) The cyclization itself requires formation of a higly Lewis acidic central fragment, which in turn leads to strong intramolecular interaction, so promoting the cyclization process.

Experimental

General procedures

All air- and moisture-sensitive manipulations were carried out under an argon atmosphere using standard Schlenk tube techniques. All solvents were dried by standard procedures and distilled prior to use. ^{1}H, ^{13}C NMR spectra were recorded on Bruker 500 Avance or Bruker 400 MHz spectrometers, using a 5 mm tuneable broadband probe. Appropriate chemical shifts in ^{1}H and ^{13}C NMR spectra were related to the residual signals of the solvent ($CDCl_3$: $\delta(^1H)$ = 7.27 ppm and $\delta(^{13}C)$ = 77.23 ppm, C_6D_6: $\delta(^1H)$ = 7.16 ppm). ^{31}P NMR spectra were relative to external H_3PO_4 ($\delta(^{31}P)$ = 0.00 ppm) The positive- and negative-ion electrospray ionization (ESI) mass spectra were measured on an ion trap analyzer Esquire 3000 (Bruker Daltonics, Bremen, Germany) in the range m/z 50–1000. The samples were dissolved in acetonitrile and analyzed by direct infusion at a flow rate of 3 μL min^{-1}. The ion source temperature was 300 °C, the tuning parameter compound stability was 100%, the flow rate and the pressure of nitrogen were 4 l min^{-1} and 10 psi, respectively. The starting compounds: AgO_3SCF_3 (99%), PCl_3 (99.999%), $AsCl_3$ (99.99%), $SbCl_3$ (99.999%) and $BiCl_3$ (99.999%), were obtained from commercial suppliers and used as delivered. The ligands L^{1-4} were prepared according to published works or by analogous procedures.[13,18,21a] $AgCB_{11}H_{12}$ was prepared according to the method of Reed.[29]

Syntheses

Synthesis of [2-(OCH$_2$)-6-(Me$_2$NCH$_2$)C$_6$H$_3$]PCl (1). A hexane solution of *n*-BuLi (1.6 mL, 2.49 mmol, 1.6 M solution) was added to a solution of L^4H (0.55 g, 2.49 mmol) in hexane (30 mL) and stirred for 3 h. The resulting orange solution of L^4Li was added to a pre-cooled solution (–80 °C) of PCl_3 (0.34 g, 0.22 mL, 2.49 mmol) in toluene (20 mL). The reaction mixture was stirred for 12 h at r.t. and the reaction mixture was filtered and the residual solid was washed with hexane (10 mL). The filtrate was evaporated *in vacuo* and the resulting yellowish oil was characterized as **1**. Yield: 0.43 g (75%). Anal. Calc. for $C_{12}H_{16}ClPO_2$ (MW 258.69): C, 55.7; H, 6.2. Found: C, 55.5; H, 6.4%. ^{1}H NMR (500 MHz, C_6D_6): δ 2.07 (6H, s, $(CH_3)_2N$), 3.23 (2H, s (br), NCH_2), 5.10 (2H, s (br), $POCH_2$), 6.78 (2H, m, Ar-H), 7.04 (1H, br, Ar-H). ^{31}P NMR (161.98 MHz, C_6D_6): δ 165.9.

Synthesis of [2,6-(MeOCH$_2$)$_2$C$_6$H$_3$]$_2$AsCl (2). A hexane solution of *n*-BuLi (4.1 mL, 6.44 mmol, 1.6 M solution) was added to a pre-cooled solution (–70 °C) of L^1Br (1.58 g, 6.44 mmol) in Et_2O (30 mL) and stirred for 2 h at this temperature. The resulting orange solution of L^1Li was added to a solution of $AsCl_3$ (0.59 g, 0.27 mL, 3.22 mmol) in Et_2O (20 mL) at –70 °C. The reaction mixture was stirred for 24 h at r.t. and evaporated *in vacuo*. The residue was extracted with toluene (30 mL) and evaporated to dryness. The crude product was crystallized from hexane to give **2** as colorless crystals (0.77 g, 55%), mp: 95–98 °C. Anal. Calc. for $C_{20}H_{26}ClAsO_4$ (MW 440.80): C, 54.5; H, 6.0. Found: C, 54.7; H, 6.2%. ^{1}H NMR (500 MHz, $CDCl_3$): δ 3.21 (6H, s, CH_3O), 4.48 (4H, AB pattern, OCH_2), 7.33 (3H, m, Ar-H3,4,5). ^{13}C NMR (125.76 MHz, $CDCl_3$): δ 58.0 (s, CH_3O), 74.4 (s, OCH_2), 128.2 (s, Ar-C3,5), 129.2 (s, Ar-C4), 142.0 (Ar-C1), 143.0 (s, Ar-C2,6). Positive-ion MS: m/z 405 $[M - Cl]^+$ (100%).

Synthesis of [2,6-(2′,4′,6′-Me$_3$C$_6$H$_2$OCH$_2$)$_2$C$_6$H$_3$]AsCl$_2$ (3). A hexane solution of *n*-BuLi (2.2 mL, 3.47 mmol, 1.6 M solution) was added to solution of L^2H (1.3 g, 3.47 mmol) in hexane (30 mL) and stirred for 12 h. The resulting suspension of L^2Li was added to a pre-cooled solution (–30 °C) of $AsCl_3$ (0.63 g, 0.29 mL, 3.47 mmol) in hexane (20 mL). The reaction mixture was stirred for 4 h then hexane (10 mL) was added. The suspension was filtered and the solid was extracted with $CHCl_3$ (20 mL). The extract was evaporated and washed with hexane (10 mL) to give **3** as a cream solid (0.81 g, 45%), mp 164–166 °C. Anal. Calc. for $C_{26}H_{29}Cl_2AsO_2$ (MW 519.35): C, 60.1; H, 5.6. Found: C, 60.2; H, 5.7%. ^{1}H NMR (500 MHz, $CDCl_3$): δ 2.26 (12H, s, 2,6-(CH_3) of mesityl), 2.28 (6H, s, 4-(CH_3) of mesityl), 5.35 (4H, s, OCH_2), 6.87 (4H, s, Ar-mesityl), 7.58 (1H, t, Ar-H4), 7.75 (2H, d, Ar-H3,5). ^{13}C NMR (125.76 MHz, $CDCl_3$): δ 17.1 (s, 2,6-(CH_3) of mesityl), 20.9 (s, 4-(CH_3) of mesityl), 72.5 (s, OCH_2), 128.4 (s, Ar-C3,5), 129.7 (s, mesityl-C3,5), 130.8 (s, mesityl-C2,6), 132.2 (s, Ar-C4), 134.0 (s, mesityl-C4), 141.8 (Ar-C1), 143.2 (s, Ar-C2,6), 153.9 (s, mesityl-C1). Positive-ion MS: m/z 521 $[L^2As(OH)_2 + K]^+$ (6%); m/z 505 $[L^2As(OH)_2 + Na]^+$ (27%); m/z 483 $[M - Cl]^+$ (9%); m/z 465 $[L^2As(OH)]^+$ (100%); m/z 329 $[L^2As(OH) - C_9H_{11}OH]^+$ (4%). Negative-ion MS: m/z 535 $[L^2AsCl(OH) + Cl]^-$ (100%)

Synthesis of [2-(OCH$_2$)-6-(*t*-BuOCH$_2$)C$_6$H$_3$]AsCl (4). A solution of L^3Li[30] (1.19 g, 4.64 mmol) in Et_2O (20 mL) was added to a solution of $AsCl_3$ (0.84 g, 0.39 mL, 4.64 mmol) in Et_2O (30 mL) at –70 °C. The reaction mixture was stirred for 12 h at r.t. and filtered. The filtrate was evaporated and crystallization of the residue from hexane at 0 °C gave **4** as colorless crystals (0.87 g, 62%), mp 69 °C. Anal. Calc. for $C_{12}H_{16}ClAsO_2$ (MW 302.63): C, 47.6; H, 5.3. Found: C, 47.7; H, 5.5%. ^{1}H NMR (500 MHz, $CDCl_3$): δ 1.43 (9H, s, $(CH_3)_3CO$), 4.76 (2H, s, $(CH_3)_3COCH_2$), 5.56 (2H, s (br), $AsOCH_2$), 7.20 (1H, d, Ar-H), 7.35 (1H, d, Ar-H), 7.45 (1H, dd, Ar-H). ^{13}C NMR (125.76 MHz, $CDCl_3$): δ 27.7 (s, $(CH_3)_3CO$), 62.1 (s, $(CH_3)_3COCH_2$), 76.2 (s, $(CH_3)_3COCH_2$), 77.1 (s, $AsOCH_2$), 119.9, 123.7, 130.6, 141.6, 143.1, 148.0 (s, Ar-C). Positive-ion MS: m/z 591 $[L_2As_2O + H_2O + Na]^+$ (42%); m/z 573 $[L_2As_2O + Na]^+$ (9%); m/z 551 $[L_2As_2O + H]^+$ (13%); m/z 323 $[LAs(OH) + K]^+$ (10%); m/z 307 $[LAs(OH) + Na]^+$ (100%).

Synthesis of [2-(Me$_2$NCH$_2$)-6-(*t*-BuOCH$_2$)C$_6$H$_3$]AsCl$_2$ (5). A hexane solution of *n*-BuLi (1.7 mL, 2.71 mmol, 1.6 M solution) was added to solution of L^4H (0.6 g, 2.71 mmol) in hexane (30 mL) and stirred for 3 h. The resulting orange solution of L^4Li was added to a pre-cooled solution (–60 °C) of $AsCl_3$ (0.49 g, 0.23 mL, 2.71 mmol) in hexane (20 mL). The reaction mixture was stirred for 12 h at r.t. and the reaction mixture was filtered. The remaining solid was washed with hexane and extracted with CH_2Cl_2 (20 mL). The extract was evaporated and the crude solid was crystallized from a minimum amount of CH_2Cl_2 to give **5** as colorless crystals (0.43 g, 43%), mp 166 °C (decomp.). Anal. Calc. for $C_{14}H_{22}Cl_2AsON$ (MW 366.17): C, 45.9; H, 6.1. Found:

C, 45.7; H, 6.0%. ^{1}H NMR (500 MHz, $CDCl_3$): δ 1.52 (9H, s, $(CH_3)_3CO$), 3.16 (6H, s, $(CH_3)_2N$), 4.49 (2H, s, NCH_2), 4.84 (2H, s, OCH_2), 7.17 (2H, m, Ar-H), 7.31 (1H, dd, Ar-H). ^{13}C NMR (125.76 MHz, $CDCl_3$): δ 28.1 (s, $(CH_3)_3CO$), 50.4 (s, $(CH_3)_2N$), 62.7 (s, NCH_2), 67.1 (s, OCH_2), 80.2 (s, $(CH_3)_3CO$), 123.3, 125.0, 130.5, 140.5, 141.6, 147.2 (s, Ar-C). Positive-ion MS: m/z 623 $[(L^4)_2As_2O_2 + H]^+$ (15%); m/z 352 $[L^4As(OH)_2 + Na]^+$ (10%); m/z 312 $[L^4As(OH)]^+$ (100%); m/z 296 $[L^4As(OH)_2 + Na - C_4H_8]^+$ (2%); m/z 256 $[L^4As(OH) - C_4H_8]^+$ (16%).

Synthesis of [2-(OCH_2)-6-(*t*-BuOCH_2)C_6H_3]SbCl (6).

Method A. Compound L^3SbCl_2 (50 mg, 0.11 mmol) was dissolved in dried (distilled from $LiAlH_4$) $CDCl_3$ (2 mL) and the resulting mixture was stirred in a NMR tube. The progress of the reaction was monitored by ^{1}H NMR spectroscopy. The reaction was stopped after 6 months, with the conversion of the starting compound to compound **6** in *ca*. 60%. The solvent was evaporated *in vacuo*. Compound **6** was obtained after recrystallization of the solid residue from a CH_2Cl_2–hexane mixture to give **6** (19 mg, 48%) mp 123 °C (decomp.). Anal. Calc. for $C_{12}H_{16}ClSbO_2$ (MW 349.46): C, 41.2; H, 4.6. Found: C, 41.4; H, 4.5%. ^{1}H NMR (500 MHz, $CDCl_3$): δ 1.47 (9H, s, $(CH_3)_3CO$), 4.77 (2H, s, $(CH_3)_3COCH_2$), 5.63 (2H, s (br), $SbOCH_2$), 7.16 (1H, d, Ar-H), 7.30 (1H, d, Ar-H), 7.41 (1H, dd, Ar-H). ^{13}C NMR (125.76 MHz, $CDCl_3$): δ 28.4 (s, $(CH_3)_3CO$), 63.0 (s, $(CH_3)_3COCH_2$), 75.3 (s, $(CH_3)_3COCH_2$), 78.1 (s, $SbOCH_2$), 120.9, 123.3, 130.2, 143.8, 150.1, 151.5 (s, Ar-C). Positive-ion MS: m/z 661 $[L_2Sb_2O_2H_2 + H]^+$ (100%); m/z 349 $[M + H]^+$ (10%); m/z 293 $[M + H - C_4H_8]^+$ (65%). Negative-ion MS: m/z 383 $[M + Cl]^-$ (77%); m/z 291 $[M - H - C_4H_8]^-$ (100%).

Method B. Compound **7** (30 mg, 0.05 mmol) was put into a NMR tube and dried (distilled from $LiAlH_4$) $CDCl_3$ (2 mL) was added and the resulting mixture was stirred. The progress of the reaction was monitored by ^{1}H NMR spectroscopy, showing the full conversion of **7** to **6** typically in 6 days. The ^{1}H and ^{13}C NMR data were consistent with those obtained by method A. The product was not isolated.

Synthesis of [2,6-(*t*-BuOCH_2)C_6H_3]SbCl(CF_3SO_3) (7). A mixture of L^3SbCl_2 (0.25 g, 0.56 mmol) and AgOTf (0.14 g, 0.56 mmol) in CH_2Cl_2 was stirred for 10 min. The precipitated AgCl was filtered of and the mixture was evaporated *in vacuo*. The remaining solid was washed with hexane (10 mL) and dried *in vacuo* to give **7** as a white powder (0.28 g, 88%), mp 115 °C (decomp.). Anal. Calc. for $C_{17}H_{25}ClSbSO_5F_3$ (MW 555.65): C, 36.8; H, 4.5. Found: C, 36.9; H, 4.7%. ^{1}H NMR (500 MHz, $CDCl_3$): δ 1.70 (18H, s, $(CH_3)_3CO$), 5.17 (4H, s, OCH_2), 7.28 (2H, d, Ar-H3,5), 7.46 (1H, t, Ar-H4). ^{13}C NMR (125.76 MHz, $CDCl_3$): δ 28.7 (s, $(CH_3)_3CO$), 68.0 (s, OCH_2), 87.4 (s, $(CH_3)_3CO$), 119.7 (q, CF_3, $^1J(^{13}C,^{19}F)$ = 318 Hz), 123.0 (s, Ar-C3,5), 131.1 (s, Ar-C4), 142.9 (s, Ar-C2,6), 147.7 (Ar-C1). Positive-ion MS: m/z 791 $[(L^3)_2Sb_2O_2 + H_2O + H]^+$ (24%); m/z 773 $[(L^3)_2Sb_2O_2 + H]^+$ (17%); m/z 405 $[L^3SbCl]^+$ (20%); m/z 387 $[L^3SbOH]^+$ (100%); m/z 349 $[L^3SbCl - C_4H_8]^+$ (11%); m/z 331 $[L^3SbOH - C_4H_8]^+$ (58%); m/z 313 $[L^3SbOH - C_4H_8 - H_2O]^+$ (23%); m/z 293 $[L^3SbCl - 2C_4H_8]^+$ (21%); m/z 257 $[L^3SbOH - 2C_4H_8 - H_2O]^+$ (21%). Negative-ion MS: m/z 149 $[CF_3SO_3]^-$ (100%).

Synthesis of [2-(Me_2NCH_2)-6-(*t*-BuOCH_2)C_6H_3]$SbCl_2$ (8). A hexane solution of *n*-BuLi (2.1 mL, 3.3 mmol, 1.6 M solution) was added to a solution of L^4H (0.73 g, 3.3 mmol) in hexane (30 mL) and stirred for 5 h. The resulting orange solution of L^4Li was added to a pre-cooled solution (–60 °C) of $SbCl_3$ (0.74 g, 3.3 mmol) in Et_2O (30 mL). The reaction mixture was stirred for 12 h. The volume of reaction mixture was reduced to *ca* one half and hexane (10 mL) was added. The insoluble material was collected by filtration and extracted with CH_2Cl_2 (30 mL). The extract was evaporated to dryness, washed with hexane (10 mL) and dried *in vacuo* to give **8** as a cream solid (0.83 g, 61%), mp 186 °C (decomp.). Anal. Calc. for $C_{14}H_{22}Cl_2SbON$ (MW 412.99): C, 40.7; H, 5.4. Found: C, 40.9; H, 5.5%. ^{1}H NMR (500 MHz, $CDCl_3$): δ 1.60 (9H, s, $(CH_3)_3CO$), 3.02 (6H, s, $(CH_3)_2N$), 4.39 (2H, s, NCH_2), 4.95 (2H, s, OCH_2), 7.22 (2H, m, Ar-H), 7.34 (1H, dd, Ar-H). ^{13}C NMR (125.76 MHz, $CDCl_3$): δ 28.6 (s, $(CH_3)_3CO$), 49.2 (s, $(CH_3)_2N$), 64.3 (s, NCH_2), 67.2 (s, OCH_2), 81.6 (s, $(CH_3)_3CO$), 124.6, 124.7, 129.9, 143.0, 154.9 (s, Ar-C), (Ar-C1) not observed. Positive-ion MS: m/z 398 $[L^4Sb(OH)_2 + Na]^+$ (100%); m/z 376 $[M - Cl]^+$ (31%); m/z 358 $[L^4SbOH]^+$ (12%); m/z 342 $[L^4Sb(OH)_2 + Na - C_4H_8]^+$ (7%); m/z 320 $[M - Cl - C_4H_8]^+$ (10%). Negative-ion MS: m/z 446 $[M + Cl]^-$ (100%).

Synthesis of [2-(Me_2NCH_2)-6-(*t*-BuOCH_2)C_6H_3]SbCl($CB_{11}H_{12}$) (9). $AgCB_{11}H_{12}$ (90 mg, 0.36 mmol) was added as a solid to a solution of **8** (150 mg, 0.36 mmol) in CH_2Cl_2 (10 mL) and stirred for 2 h. Than the insoluble material was filtered off and the filtrate was evaporated *in vacuo* and washed with hexane. The crude product was recrystallized from a CH_2Cl_2–hexane mixture (142 mg, 75%), mp 186 °C (decomp.). Anal. Calc. for $C_{15}H_{34}B_{11}ClSbON$ (MW 520.57): C, 34.6; H, 6.6. Found: C, 34.7; H, 6.8%. ^{1}H NMR (500 MHz, $CDCl_3$): δ 1.61 (9H, s, $(CH_3)_3CO$), 2.97 (6H, s, $(CH_3)_2N$), 4.37 (2H, s, NCH_2), 5.04 (2H, s, OCH_2), 7.39 (1H, d, Ar-H), 7.43 (1H, d, Ar-H), 7.57 (1H, dd, Ar-H). ^{13}C NMR (125.76 MHz, $CDCl_3$): δ 28.7 (s, $(CH_3)_3CO$), 47.1 (s, $(CH_3)_2N$), 52.1 (s (br), C-cage), 65.6 (s, NCH_2), 66.4 (s, OCH_2), 84.5 (s, $(CH_3)_3CO$), 125.2, 125.6, 133.1, 144.8, 144.6, 145.3 (s, Ar-C). Positive-ion MS: m/z 398 $[L^4Sb(OH)_2 + Na]^+$ (33%); m/z 376 $[L^4SbCl]^+$ (17%); m/z 358 $[L^4SbOH]^+$ (100%); m/z 342 $[L^4Sb(OH)_2 + Na - C_4H_8]^+$ (5%); m/z 320 $[L^4SbCl - C_4H_8]^+$ (8%) m/z 302 $[L^4SbOH - C_4H_8]^+$ (18%). Negative-ion MS: m/z 145 $[CB_{11}H_{12}]^-$ (100%).

Synthesis of [2-(Me_2NCH_2)-6-(*t*-BuOCH_2)C_6H_3]$BiCl_2$ (10). A hexane solution of *n*-BuLi (4.2 mL, 6.7 mmol, 1.6 M solution) was added to solution of L^4H (1.48 g, 6.7 mmol) in hexane (30 mL) and stirred for 5 h. The resulting orange solution of L^4Li was added to a pre-cooled solution (–60 °C) of $BiCl_3$ (2.11 g, 6.7 mmol) in Et_2O (60 mL). The reaction mixture was stirred for 12 h. The volume of reaction mixture was reduced to *ca*. one half and hexane (10 mL) was added. The insoluble material was collected by filtration and extracted with CH_2Cl_2 (30 mL). The extract was evaporated to dryness, washed with hexane (10 mL) and dried *in vacuo* to give **10** as a cream solid. (1.57 g, 47%), mp 228 °C (decomp.). Anal. Calc. for $C_{14}H_{22}Cl_2BiON$ (MW 500.22): C, 33.6; H, 4.4. Found: C, 33.9; H, 4.5%. ^{1}H NMR (500 MHz, $CDCl_3$): δ 1.54 (9H, s, $(CH_3)_3CO$), 3.13 (6H, s, $(CH_3)_2N$), 4.78 (2H, s, NCH_2), 5.08 (2H, s, OCH_2), 7.47 (1H, dd, Ar-H), 7.73 (1H, d, Ar-H), 7.80 (1H, d, Ar-H). ^{13}C NMR (125.76 MHz, $CDCl_3$): δ 28.7 (s, $(CH_3)_3CO$), 48.9 (s, $(CH_3)_2N$), 68.4 (s, NCH_2), 71.4 (s, OCH_2), 81.0 (s, $(CH_3)_3CO$), 127.2, 128.2, 129.2, 150.0, 152.4 (s, Ar-C), (Ar-C1) not observed. Positive-ion MS: m/z 464 $[M - Cl]^+$ (100%); m/z 408 $[M - Cl - C_4H_8]^+$ (10%). Negative-ion MS: m/z 534 $[M + Cl]^-$ (100%).

Synthesis of [2-(Me_2NCH_2)-6-(*t*-$BuOCH_2$)C_6H_3]BiCl(CF_3SO_3) (11). Analogously to the procedure described for **9**. AgOTf (119 mg, 0.46 mmol) and **10** (230 mg, 0.46 mmol). (**11**, 166 mg, 59%), mp 171–174 °C. Anal. Calc. for $C_{15}H_{22}ClF_3BiO_4NS$ (MW 613.84): C, 29.4; H, 3.6. Found: C, 29.6; H, 3.7%. ^{1}H NMR (500 MHz, $CDCl_3$): δ 1.61 (9H, s, $(CH_3)_3CO$), 3.11 (6H, s, $(CH_3)_2N$), 4.77 (2H, s, NCH_2), 5.16 (2H, s, OCH_2), 7.59 (1H, dd, Ar-H), 7.84 (1H, d, Ar-H), 7.92 (1H, d, Ar-H). ^{13}C NMR (125.76 MHz, $CDCl_3$): δ 28.5 (s, $(CH_3)_3CO$), 48.4 (s (br), $(CH_3)_2N$), 69.0 (s, NCH_2), 71.1 (s, OCH_2), 82.1 (s, $(CH_3)_3CO$), 119.3 (q, CF_3, $^1J(^{13}C,^{19}F)$ = 320 Hz), 127.3, 128.4, 130.4, 151.2, 153.4 (s, Ar-C), (Ar-C1) not observed. Positive-ion MS: *m*/*z* 464 $[L^4BiCl]^+$ (100%); *m*/*z* 408 $[L^4BiCl - C_4H_8]^+$ (69%). Negative-ion MS: *m*/*z* 149 $[CF_3SO_3]^-$ (100%).

Synthesis of [2-(Me_2NCH_2)-6-(*t*-$BuOCH_2$)C_6H_3]BiCl($CB_{11}H_{12}$) (12). Analogously to the procedure described for **9**. $AgCB_{11}H_{12}$ (88 mg, 0.35 mmol) and **10** (175 mg, 0.35 mmol). (**12**, 115 mg, 63%), mp 205 °C (decomp.). Anal. Calc. for $C_{15}H_{34}ClB_{11}BiON$ (MW 520.57): C, 34.6; H, 6.6. Found: C, 34.7; H, 6.8%. ^{1}H NMR (500 MHz, $CDCl_3$): δ 1.59 (9H, s, $(CH_3)_3CO$), 3.11 (6H, s, $(CH_3)_2N$), 4.84 (2H, s, NCH_2), 5.17 (2H, s, OCH_2), 7.68 (1H, dd, Ar-H), 7.91 (1H, d, Ar-H), 8.04 (1H, d, Ar-H). ^{13}C NMR (125.76 MHz, $CDCl_3$): δ 28.6 (s, $(CH_3)_3CO$), 47.9 (s, $(CH_3)_2N$), 53.1 (s (br), C-cage), 69.3 (s, NCH_2), 71.5 (s, OCH_2), 83.1 (s, $(CH_3)_3CO$), 127.7, 129.0, 131.3, 151.4, 153.9 (s, Ar-C), (Ar-C1) not observed. Positive-ion MS: *m*/*z* 464 $[L^4BiCl]^+$ (100%); *m*/*z* 408 $[L^4BiCl - C_4H_8]^+$ (94%). Negative-ion MS: *m*/*z* 145 $[CB_{11}H_{12}]^-$ (100%).

X-Ray crystallography

Suitable single crystals were mounted on glass fibre with oil and measured on four-circle diffractometer KappaCCD with CCD area detector by monochromatized Mo-Kα radiation (λ = 0.71073 Å) at 150(1) K. Numerical[31] absorption corrections from crystal shape were applied for all crystals. The structures were solved by the direct method (SIR92)[32] and refined by a full-matrix least-squares procedure based on F^2 (SHELXL97)[33] Hydrogen atoms were fixed into idealized positions (riding model) and assigned temperature factors U_{iso}(H) = 1.2U_{eq} (pivot atom) or of 1.5U_{eq} for the methyl moiety with C–H = 0.96, 0.97 and 0.93 Å for methyl, methylene and hydrogen atoms in aromatic ring, respectively. The final difference maps displayed no peaks of chemical significance, as the highest peaks and holes are in close vicinity (~ 1 Å) of the heavy atoms, in the case of compounds **3–5**, **7** and **8**. Two independent molecules were observed in the asymmetric unit cell of **2**. One of the coordinating arms of one of the molecules is strongly disordered. It was not possible to model this disordered group with a satisfactory result, nevertheless the second molecule was well modeled. There is disordered solvent (dichloromethane) in the small, porous and weakly diffracting crystal of **6**. Attempts were made to model this disorder or split it into two positions but this was unsuccessful. PLATON/SQUEEZE[34] was used to correct the data for the presence of disordered solvent. A potential solvent volume of 852 Å^3 was found. 433 electrons per unit cell worth of scattering were located in the void. The calculated stoichiometry of solvent was calculated to be ten additional molecules of dichloromethane per unit cell which results in 420 electrons per unit cell. The C–H group within the carborane cage in the structure of **9** was placed by the help of C–B and B–B interatomic distances comparison. There are large electron density maxima in close proximity of the Bi atom in **10**, **11** and **12**. This is probably due to the application of an improper absorption correction method. We tried different possible methods but the best result obtained for this parameter is still unsatisfactorily high. In the case of bismuth compounds the location of the maxima, which have no chemical significance, we think is not a serious problem.

Crystallographic data for 2. $2(C_{20}H_{26}AsClO_4)$, *M* = 881.56, orthorhombic, $Pna2_1$, *a* = 17.0370(5), *b* = 7.618(2), *c* = 31.5390(14) Å, *V* = 4093.4(13) Å^3, *Z* = 4, *T* = 150(1) K, 17720 total reflections, 8315 independent (R_{int} = 0.051, *R*1 (obs. data) = 0.062, wR_2 (all data) 0.125).

Crystallographic data for 3. $C_{26}H_{29}AsCl_2O_2$), *M* = 519.31, triclinic, $P\bar{1}$, *a* = 8.0719(6), *b* = 11.9821(9), *c* = 13.1989(6) Å, α = 80.579(5), β = 79.169(4), γ = 79.737(7)°, *V* = 1222.53(14) Å^3, *Z* = 2, *T* = 150(1) K, 22718 total reflections, 5590 independent (R_{int} = 0.036, *R*1 (obs. data) = 0.036, wR_2 (all data) 0.075).

Crystallographic data for 4. $C_{12}H_{16}AsClO_2$, *M* = 302.62, monoclinic, *C*2/*c*, *a* = 25.3962(7), *b* = 8.1221(9), *c* = 14.6069(12) Å, β = 116.012(7), *V* = 2707.7(4) Å^3, *Z* = 8, *T* = 150(1) K, 10758 total reflections, 3091 independent (R_{int} = 0.134, *R*1 (obs. data) = 0.067, wR_2 (all data) 0.087).

Crystallographic data for 5. $C_{14}H_{22}AsCl_2ON$, *M* = 366.15, monoclinic, $P2_1/c$, *a* = 11.2757(8), *b* = 10.3700(4), *c* = 16.1121(16) Å, β = 121.939(6), *V* = 1598.8(2) Å^3, *Z* = 4, *T* = 150(1) K, 14207 total reflections, 3642 independent (R_{int} = 0.043, *R*1 (obs. data) = 0.041, wR_2 (all data) 0.085).

Crystallographic data for 6. $C_{48}H_{64}Sb_4Cl_4O_8 \cdot 4.5CH_2Cl_2$ *M* = 1779.96, monoclinic, $P2_1/c$, *a* = 18.544(2), *b* = 19.350(2), *c* = 26.135(3) Å, β = 134.565(12), *V* = 6681.3(14) Å^3, *Z* = 4, *T* = 150(1) K, 81089 total reflections, 13081 independent (R_{int} = 0.059, *R*1 (obs. data) = 0.053, wR_2 (all data) 0.105).

Crystallographic data for 7. $C_{16}H_{25}SbClO_2 \cdot CF_3SO_3$, *M* = 555.63, monoclinic, $P2_1/c$, *a* = 9.3050(10), *b* = 12.4460(12), *c* = 19.4031(14) Å, β = 104.615(6), *V* = 2174.4(4) Å^3, *Z* = 4, *T* = 150(1) K, 17557 total reflections, 4950 independent (R_{int} = 0.045, *R*1 (obs. data) = 0.036, wR_2 (all data) 0.069).

Crystallographic data for 8. $C_{14}H_{22}SbCl_2ON$, *M* = 412.98, monoclinic, $P2_1/c$, *a* = 11.525(4), *b* = 10.5691(13), *c* = 16.038(3) Å, β = 122.680(18), *V* = 1644.3(7) Å^3, *Z* = 4, *T* = 150(1) K, 12117 total reflections, 3748 independent (R_{int} = 0.034, *R*1 (obs. data) = 0.033, wR_2 (all data) 0.075).

Crystallographic data for 9. $C_{14}H_{22}SbClON \cdot CB_{11}H_{12} \cdot CH_2Cl_2$ *M* = 605.47, triclinic, $P\bar{1}$, *a* = 9.5870(3), *b* = 12.0591(6), *c* = 13.2669(6) Å, α = 65.008(5), β = 88.935(4), γ = 84.972(3)°, *V* = 1384.54(12) Å^3, *Z* = 2, *T* = 150(1) K, 29624 total reflections, 6648 independent (R_{int} = 0.020, *R*1 (obs. data) = 0.023, wR_2 (all data) 0.059).

Crystallographic data for 10. $C_{14}H_{22}BiCl_2ON$, *M* = 500.21, monoclinic, $P2_1/c$, *a* = 9.21985(4), *b* = 11.7940(7), *c* = 17.0903(11) Å, β = 112.714(4), *V* = 1714.25(16) Å^3, *Z* = 4, *T* = 150(1) K, 12032 total reflections, 3853 independent (R_{int} = 0.042, *R*1 (obs. data) = 0.042, wR_2 (all data) 0.093).

Crystallographic data for 11. $C_{14}H_{22}BiClON{\cdot}CF_3SO_3$, M = 613.83, triclinic, $P\bar{1}$, a = 7.7441(5), b = 11.0320(8), c = 12.5790(8) Å, α = 74.564(5), β = 85.146(5), γ = 74.351(5)°, V = 997.39(12) Å^3, Z = 2, T = 150(1) K, 18498 total reflections, 4494 independent (R_{int} = 0.087, $R1$ (obs. data) = 0.079, wR_2 (all data) 0.192).

Crystallographic data for 12. $C_{14}H_{22}BiClON{\cdot}CB_{11}H_{12}{\cdot}2CH_2Cl_2$, M = 777.62, triclinic, $P\bar{1}$, a = 9.1429(7), b = 11.9780(4), c = 15.2951(9) Å, α = 71.583(6), β = 81.044(6), γ = 87.254(7)°, V = 1569.86(17) Å^3, Z = 2, T = 150(1) K, 27420 total reflections, 7142 independent (R_{int} = 0.031, $R1$ (obs. data) = 0.030, wR_2 (all data) 0.070).

Acknowledgements

The authors thank the Grant agency of the Czech Republic project no. P207/10/0215 and the Ministry of Education of the Czech Republic (projects MSM0021627501) for financial support. R. Jirásko acknowledges the support of grant project No. MSM0021627502 sponsored by The Ministry of Education, Youth and Sports of the Czech Republic. F. D. P. wishes to acknowledge the Research Foundation Flanders (FWO) and the Free University of Brussels (VUB) for continuous support to his research group.

Notes and references

1 G. van Koten, *Pure Appl. Chem.*, 1989, **61**, 1681.
2 For several examples, see: (*a*) M. Albrecht and G. van Koten, *Angew. Chem., Int. Ed.*, 2001, **40**, 3750; (*b*) M. E. van der Boom and D. Milstein, *Chem. Rev.*, 2003, **103**, 1759; (*c*) *The Chemistry of Pincer Compounds*, ed. D. Morales-Morales and C. M. Jensen, Elsevier, Amsterdam, 2007; (*d*) I. Moreno, R. SanMartin, B. Ines, M. T. Herrero and E. Domínguez, *Curr. Org. Chem.*, 2009, **13**, 878; (*e*) D. Milstein, *Top. Catal.*, 2010, **53**, 915.
3 For most recent examples, see: (*a*) J. A. Thagfi, S. Dastgir, A. J. Lough and G. G. Lavoie, *Organometallics*, 2010, **29**, 3133; (*b*) D. M. Spasyuk and D. Zargarian, *Inorg. Chem.*, 2010, **49**, 6203; (*c*) B. M. J. M. Suijkerbuijk, D. J. Schamhart, H. Kooijman, A. L. Spek, G. van Koten and R. J. M. K. Gebbink, *Dalton Trans.*, 2010, **39**, 6198.
4 For most recent examples, see: (*a*) R. Gerber, T. Fox and C. M. Frech, *Chem.–Eur. J.*, 2010, **16**, 6771; (*b*) E. Sola, A. García-Camprubi, J. L. André, M. Martín and P. Plou, *J. Am. Chem. Soc.*, 2010, **132**, 9111; (*c*) E. Khaskin, M. A. Iron, L. J. W. Shimon, J. Zhang and D. Milstein, *J. Am. Chem. Soc.*, 2010, **132**, 8542.
5 (*a*) M. J. Paget, J. Wagler and B. A. Messerle, *Organometallics*, 2010, **29**, 3790; (*b*) S. Bonnet, M. Lutz, A. L. Spek, G. van Koten and R. J. M. K. Gebbink, *Organometallics*, 2010, **29**, 1157; (*c*) V. A. Kozlov, D. V. Aleksanyan, Y. V. Nelyubina, K. A. Lyssenko, E. I. Gutsul, A. A. Vasilev, P. V. Petrovskii and I. L. Odinets, *Dalton Trans.*, 2009, 8657; (*d*) J. Aydin, N. Selander and K. J. Szabó, *Tetrahedron Lett.*, 2006, **47**, 8999; (*e*) M. A. Amiri, P. Meunier, R. Louis, N. Pirio and H. Ossor, *Phosphorus, Sulfur Silicon Relat. Elem.*, 2000, **156**, 1; (*f*) C. A. Kruithof, A. Berger, P. H. Dijkstra, F. Soulimani, T. Visser, M. Lutz, A. L. Spek, R. J. M. K. Gebbink and G. van Koten, *Dalton Trans.*, 2009, 3306; (*g*) D. Pugh and A. A. Danopoulos, *Coord. Chem. Rev.*, 2007, **251**, 610.
6 M. Mehring, M. Schürmann and K. Jurkschat, *Organometallics*, 1998, **17**, 1227.
7 For example see: (*a*) K. Peveling, M. Schürmann and K. Jurkschat, *Z. Anorg. Allg. Chem.*, 2002, **628**, 2435; (*b*) V. Deáky, M. Schürmann and K. Jurkschat, *Z. Anorg. Allg. Chem.*, 2009, **635**, 1380; (*c*) M. Henn, M. Schürmann, B. Mahieu, P. Zanello, A. Cinquantini and K. Jurkschat, *J. Organomet. Chem.*, 2006, **691**, 1560; (*d*) K. Peveling, K. Dannappel, M. Schürmann, B. Costisella and K. Jurkschat, *Organometallics*, 2006, **25**, 368; (*e*) K. Dannappel, M. Schürmann, B. Costisella and K. Jurkschat, *Organometallics*, 2004, **24**, 1032.
8 (*a*) K. Peveling, M. Henn, C. Low, M. Mehring, M. Schürmann, B. Costisella and K. Jurkschat, *Organometallics*, 2004, **23**, 1501; (*b*) M. Mehring, I. Vrasidas, D. Horn, M. Schürmann and K. Jurkschat, *Organometallics*, 2001, **20**, 4647; (*c*) K. Peveling, M. Schürmann, R. Ludwig and K. Jurkschat, *Organometallics*, 2001, **20**, 4654; (*d*) M. Mehring, C. Low, M. Schürmann and K. Jurkschat, *Eur. J. Inorg. Chem.*, 1999, 887.
9 (*a*) S. Sarkar, A. R. Carlson, M. K. Veige, J. M. Falkowski, K. A. Abboud and A. S. Veige, *J. Am. Chem. Soc.*, 2008, **130**, 1116; (*b*) S. Kuppuswamy, A. J. Peloquin, I. Ghiviriea, K. A. Abboud and A. S. Veige, *Organometallics*, 2010, **29**, 4227.
10 J. Vicente, A. Arcas and M. D. Gálvez-López, *Organometallics*, 2004, **23**, 3521.
11 (*a*) M. Gandelman, A. Vigalok, L. J. W. Shimon and D. Milstein, *Organometallics*, 1997, **16**, 3981; (*b*) M. Gandelman, L. Konstantinovski, H. Rozenberg and D. Milstein, *Chem.–Eur. J.*, 2003, **9**, 2595; (*c*) M. Gandelman, B. Rybtchinski, N. Ashkenazi, R. M. Gauvin and D. Milstein, *J. Am. Chem. Soc.*, 2001, **123**, 5372; (*d*) B. Rybtchinski, S. Oevers, M. Montag, A. Vigalok, H. Rozenberg, J. M. L. Martin and D. Milstein, *J. Am. Chem. Soc.*, 2001, **123**, 9064; (*e*) J. Fischer, M. Schürmann, M. Mehring, V. Zachwieja and K. Jurkschat, *Organometallics*, 2006, **25**, 2886.
12 (*a*) V. A. Kozlov, D. V. Aleksanyan, Y. V. Nelyubina, K. A. Lyssenko, A. A. Vasil'ev, P. V. Petrovskii and I. L. Odinest, *Organometallics*, 2010, **29**, 2054; (*b*) A. Choualeb, A. J. Lough and D. G. Gusev, *Organometallics*, 2007, **26**, 5224; (*c*) V. Gomez-Benitez, R. A. Toscano and D. Morales-Morales, *Inorg. Chem. Commun.*, 2007, **10**, 1; (*d*) E. Poverenov, M. Gandelman, L. J. W. Shimon, H. Rozenberg, Y. Ben-David and D. Milstein, *Organometallics*, 2005, **24**, 1082; (*e*) G. R. Fulmer, W. Kaminski, R. A. Kemp and K. I. Goldberg, *Organometallics*, 2011, **30**, 1627.
13 R. Jambor, L. Dostál, A. Růžička, I. Císařová, J. Brus and J. Holeček, *Organometallics*, 2002, **21**, 3996.
14 For example, see: (*a*) L. Dostál, I. Císařová, R. Jambor, A. Růžička, R. Jirásko and J. Holeček, *Organometallics*, 2006, **25**, 4366; (*b*) L. Dostál, R. Jambor, A. Růžička, I. Císařová and J. Holeček, *Appl. Organomet. Chem.*, 2005, **19**, 797; (*c*) B. Kašná, R. Jambor, L. Dostál, I. Císařová, J. Holeček and B. Štíbr, *Organometallics*, 2006, **25**, 5139; (*d*) L. Dostál, R. Jambor, A. Růžička, A. Lyčka, J. Brus and F. de Proft, *Organometallics*, 2008, **27**, 6059; (*e*) L. Dostál, R. Jambor, A. Růžička, R. Jirásko, V. Lochař, L. Beneš and F. de Proft, *Inorg. Chem.*, 2009, **48**, 10495; (*f*) L. Dostál, R. Jambor, A. Růžička, R. Jirásko, I. Císařová and J. Holeček, *J. Fluorine Chem.*, 2008, **129**, 167; (*g*) L. Dostál, unpublished results.
15 L. Dostál, R. Jambor, A. Růžička, I. Císařová and J. Holeček, *Main Group Met. Chem.*, 2004, **27**, 291.
16 L. Dostál, P. Novák, R. Jambor, A. Růžička, I. Císařová, R. Jirásko and J. Holeček, *Organometallics*, 2007, **26**, 2911.
17 R. Jirásko and M. Holčapek, *Mass Spectrom. Rev.*, 2011, DOI: 10.1002/mas.20309.
18 M. Chovancová, R. Jambor, A. Růžička, R. Jirásko, I. Císařová and L. Dostál, *Organometallics*, 2009, **28**, 1934.
19 (*a*) M. Yoshifuji, M. Nakazawa, T. Sato and K. Toyota, *Tetrahedron*, 2000, **56**, 43; (*b*) K. Toyota, S. Kawasaki and M. Yoshifuji, *Tetrahedron Lett.*, 2002, **43**, 7953.
20 T. Řezníček, L. Dostál, A. Růžička, R. Jirásko and R. Jambor, *Inorg. Chim. Acta*, 2010, **363**, 3302.
21 (*a*) J. Vrána, R. Jambor, A. Růžička, J. Holeček and L. Dostál, *Collect. Czech. Chem*; (*b*) D. A. Atwood, A. H. Cowley and J. Ruiz, *Inorg. Chim. Acta*, 1992, **198–200**, 271; (*c*) A. P. Soran, C. Silvestru, H. J. Breunig, G. Balazs and J. C. Green, *Organometallics*, 2007, **26**, 1196.
22 L. Dostál, R. Jambor, R. Jirásko, Z. Padělková, A. Růžička and J. Holeček, *J. Organomet. Chem.*, 2010, **695**, 392.
23 I. J. Casely, J. W. Ziller, B. J. Mincher and W. J. Evans, *Inorg. Chem.*, 2011, **50**, 1513.
24 (*a*) A. D. Becke, *J. Chem. Phys.*, 1993, **98**, 5648; (*b*) C. Lee, W. Yang and R. G. Parr, *Phys. Rev. B*, 1988, **37**, 785; (*c*) P. J. Stephens, F. J. Devlin, C. F. Chabalowski and M. J. Frisch, *J. Phys. Chem.*, 1994, **98**, 11623.
25 Hydrogen and first-row: R. A. Kendall, T. H. Dunning and R. J. Harrison, *J. Chem. Phys.*, 1992, **96**, 6796; 2nd row: D. E. Woon and T. H. Dunning, *J. Chem. Phys.*, 1993, **98**, 1358; 3rd row: A. K. Wilson, D. E. Woon, K. A. Peterson and T. H. Dunning Jr., *J. Chem. Phys.*, 1999, **110**, 7667.
26 K. A. Peterson, *J. Chem. Phys.*, 2003, **119**, 11099.
27 M. J. Frisch, G. W. Trucks, H. B. Schlegel, G. E. Scuseria, M. A. Robb, J. R. Cheeseman, G. Scalmani, V. Barone, B. Mennucci, G. A. Petersson, H. Nakatsuji, M. Caricato, X. Li, H. P. Hratchian, A. F. Izmaylov, J. Bloino, G. Zheng, J. L. Sonnenberg, M. Hada, M. Ehara, K. Toyota, R. Fukuda, J. Hasegawa, M. Ishida, T. Nakajima, Y. Honda, O. Kitao, H. Nakai, T. Vreven, J. A. Montgomery, Jr., J. E. Peralta, F. Ogliaro,

M. Bearpark, J. J. Heyd, E. Brothers, K. N. Kudin, V. N. Staroverov, R. Kobayashi, J. Normand, K. Raghavachari, A. Rendell, J. C. Burant, S. S. Iyengar, J. Tomasi, M. Cossi, N. Rega, J. M. Millam, M. Klene, J. E. Knox, J. B. Cross, V. Bakken, C. Adamo, J. Jaramillo, R. Gomperts, R. E. Stratmann, O. Yazyev, A. J. Austin, R. Cammi, C. Pomelli, J. Ochterski, R. L. Martin, K. Morokuma, V. G. Zakrzewski, G. A. Voth, P. Salvador, J. J. Dannenberg, S. Dapprich, A. D. Daniels, O. Farkas, J. B. Foresman, J. V. Ortiz, J. Cioslowski and D. J. Fox, *GAUSSIAN 09 (Revision B.1)*, Gaussian, Inc., Wallingford, CT, 2009.

28 (*a*) J. P. Foster and F. Weinhold, *J. Am. Chem. Soc.*, 1980, **102**, 7211; (*b*) A. E. Reed and F. Weinhold, *J. Chem. Phys.*, 1983, **78**, 4066; (*c*) A. E. Reed, R. B. Weinstock and F. Weinhold, *J. Chem. Phys.*, 1985, **83**, 735; (*d*) A. E. Reed, L. A. Curtiss and F. Weinhold, *Chem. Rev.*, 1988, **88**, 899; (*e*) F. Weinhold, in, *Encyclopedia of Computational Chemistry*, ed. P. v. R. Schleyer, N. L. Allinger, T. Clark, J. Gasteiger, P. A. Kollman, H. F. Schaefer III and P. R. Schreiner, John Wiley & Sons, Chichester, UK, 1998, vol. 3, pp. 1792–1811.

29 K. Shelly, D. C. Finster, Y. J. Lee, W. R. Sheidt and C. A. Reed, *J. Am. Chem. Soc.*, 1985, **107**, 5955.

30 R. Jambor, L. Dostál, A. Růžička, I. Císařová and J. Holeček, *Inorg. Chim. Acta*, 2005, **358**, 2422.

31 P. Coppens, in *Crystallographic Computing*, ed. F. R. Ahmed, S. R. Hall and C. P. Huber, Copenhagen, Munksgaard, 1970, pp. 255–270.

32 A. Altomare, G. Cascarone, C. Giacovazzo, A. Guagliardi, M. C. Burla, G. Polidori and M. Camalli, *J. Appl. Crystallogr.*, 1994, **27**, 1045.

33 G. M. Sheldrick, *SHELXL-97*, A Program for Crystal Structure Refinement, University of Göttingen, Germany, 1997.

34 A. L. Spek, *Acta Crystalllogr.. Sect. A*, 1990, **46**, C34.

